Origin of Reproducibility in the Responses of Retinal Rods to Single Photons

F. Rieke*# and D. A. Baylor#

*Department of Physiology and Biophysics, University of Washington, Seattle, Washington 98195 and #Department of Neurobiology, Stanford University, Stanford, California 94305 USA

ABSTRACT The single photon responses of retinal rod cells are remarkably reproducible, allowing the number and timing of photon absorptions to be encoded accurately. This reproducibility is surprising because the elementary response arises from a single rhodopsin molecule, and typically signals from single molecules display large intertrial variations. We have investigated the mechanisms that make the rod's elementary response reproducible. Our experiments indicate that reproducibility cannot be explained by saturation within the transduction cascade, by Ca^{2+} feedback, or by feedback control of rhodopsin shutoff by any known element of the cascade. We suggest instead that deactivation through a series of previously unidentified transitions allows the catalytic activity of a single rhodopsin molecule to decay with low variability. Two observations are consistent with this view. First, the time course of rhodopsin's catalytic activity could not be accounted for by the time required for the known steps in rhodopsin deactivation—phosphorylation and arrestin binding. Second, the variability of the elementary response increased when phosphorylation was made rate-limiting for rhodopsin shutoff.

INTRODUCTION

This work examines the mechanism that enables retinal rod cells to register single photon absorptions with macroscopic signals of constant size and shape. Constancy of the elementary response is essential if the number and timing of photon absorptions are to be accurately represented. The classic frequency of seeing experiments of Hecht et al. (1942) and van der Velden (1946) established that the human visual system can detect the absorption of a few photons and that individual rods can successfully detect single photons. More recent work by Sakitt (1972) suggests that the visual system can literally count photon absorptions beginning at one or two, requiring the rods to encode accurate information about the number of absorbed photons. Photon counting would not be possible if the rod's elementary response fluctuated widely, as small responses would not be sensed by central neurons and large responses would mimic the effect of multiple photon absorptions. Variations in the shape of the elementary response would also degrade information about the timing of photon absorption and thus impair the temporal precision of rod vision. As photon absorptions occur rarely in each rod over much of the intensity range of rod vision, accurate registration of the number and timing of photon absorptions is important for normal rod vision.

It is well known that reliable photon detection requires amplification and low dark noise. The amplification is achieved by the cascade diagrammed in Fig. 1 (reviewed by Pugh and Lamb, 1993). An effective photon absorption photoisomerizes a rhodopsin molecule, which becomes catalytically active. A photoisomerized rhodopsin activates thousands of copies of the G-protein transducin (T), each of which can activate a catalytic subunit of phosphodiesterase (PDE). An activated PDE subunit typically hydrolyzes at least 50 cyclic guanosine monophosphate (cGMP) molecules (Pugh and Lamb, 1993; Rieke and Baylor, 1996). The resulting reduction in the cGMP concentration allows hundreds of cationic channels in the surface membrane to close, preventing more than 10^6 cations from entering the outer segment. This macroscopic decrease in inward current hyperpolarizes the cell membrane and slows transmitter release from the synaptic terminal. Dark noise in the transduction current arises primarily from thermal isomerization of rhodopsin and from spontaneous activation of PDE (Baylor et al., 1980; Rieke and Baylor, 1996). Although the dark noise is relatively low, it appears to limit the absolute sensitivity of vision (Aho et al., 1988).

The first evidence for the reproducibility of the rod's elementary electrical response came from statistical analysis of the photocurrents evoked by dim flashes (Baylor et al., 1979b, 1984), which revealed that the standard deviation of the response amplitude was only ~20% of the mean and that the time course was nearly fixed. The molecular mechanism of this reproducibility is intriguing because the signals generated by many types of single particles show large intertrial fluctuations. Familiar examples are the amount of charge transferred during an ion channel's open time and the time required for the decay of a radioactive atom. Such fluctuations arise from stochastic variations in the active lifetime of the particle. The rod's elementary response should reflect variability in the timing of rhodopsin deactivation because rhodopsin drives the amplifying cascade while it remains active. Yet the fluctuations in the elementary response are remarkably small. This might be explained in either of two ways: 1) the elementary response might be insensitive to variations in rhodopsin's active lifetime, or 2)

Received for publication 26 March 1998 and in final form 7 July 1998.

Address reprint requests to Dr. Fred Rieke, Department of Physiology and Biophysics, Box 357290, University of Washington, Seattle, WA 98195. Tel.: 206-616-6956; Fax: 206-685-0619; E-mail: rieke@u.washington.edu.

0006-3495/98/10/1836/22 $2.00

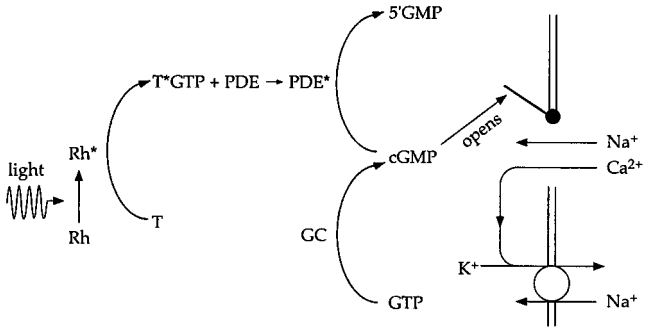

FIGURE 1 Diagram of phototransduction cascade. Effective absorption of a photon activates the photopigment rhodopsin (Rh); the cascade amplifies rhodopsin's activity to create a macroscopic electrical response. Active rhodopsin catalyzes the activation of the G protein transducin (T), which in turn activates phosphodiesterase (PDE). Activated PDE hydrolyzes cGMP, causing its concentration to fall, channels in the surface membrane to close, and the current flowing into the outer segment to decrease. The cGMP concentration and dark current are restored by cGMP synthesis by guanylate cyclase (GC). The recovery of the flash response is accelerated by Ca^{2+} feedback. Ca^{2+} enters the cell through the cGMP-gated channels and is extruded by Na^+/K^+, Ca^{2+} exchange. Influx of Ca^{2+} slows during the light response while efflux continues, causing the internal Ca^{2+} concentration to drop. The fall in Ca^{2+} concentration increases the rate of cGMP synthesis and thus speeds the return of the cGMP concentration and current to their respective dark values.

the active lifetime might have low variability. We present evidence favoring the second possibility and explore the contributions of several mechanisms.

MATERIALS AND METHODS

The experiments were carried out on isolated rods from the dark-adapted retina of the toad *Bufo marinus*, as described by Rieke and Baylor (1996). Single rods were isolated by shredding a small piece of retina, and their membrane current was recorded with a suction electrode (Baylor et al., 1979a). Experiments were performed on intact cells or on truncated, internally dialyzed outer segments. In either case, membrane current collected by the suction electrode was amplified, low-pass filtered at 20 Hz (−3 dB point; 8-pole Bessel low-pass), and digitized at 100 Hz. Light responses were elicited by 10-ms flashes of 500-nm light; the flash strength was controlled with calibrated neutral density filters. The cell was usually positioned in the suction electrode to collect as much dark current as possible. In some experiments the contribution of cellular dark noise to the measured current was minimized by drawing only the tip of the outer segment into the suction electrode and applying the stimulating flash as a transverse slit 10 μm wide. The transverse slit was also used in experiments on truncated outer segments because the shape of the response depended on the longitudinal distance from the site of truncation; in these experiments the center of the slit was positioned ~20 μm from the cut end of the outer segment. In all experiments a half-saturating response was measured periodically to check the stability of the cell, and the experiment was terminated if the response changed significantly.

Table 1 gives the compositions of the solutions. Solution changes were usually achieved with a series of electronically controlled pinch valves (Biochem Valves, Boonton, NJ) whose outlets were connected to a common perfusion pipe ~100 μm in diameter. Solution changes with this system were completed in 200–300 ms, as judged by junction potential measurements. In measurements of rhodopsin's catalytic activity (Fig. 7), faster solution changes were achieved by moving the interface between two continuously flowing solutions across the outer segment. Solutions were driven by positive pressure through a pair of glass pipes with openings ~50 μm in diameter; the pipes were mounted on a piezoelectric translation stage (Burleigh Instruments, Fishers, NY). Solution changes at the cut end of the outer segment were completed in less than 10 ms with this system.

TABLE 1 Solutions

	HEPES Ringer's	Bicarbonate Ringer's	Truncation dialysis	Truncation electrode	Ca^{2+} clamp
NaCl (mM)	120	87	—	120	—
KCl	2	2	—	—	—
$NaHCO_3$	2	35	—	—	—
$CaCl_2$	1	1	0.75	0.05	0.25
$MgCl_2$	1.6	1.6	1.6	1.6	—
Glucose	10	10	—	—	—
Hepes	3	3	3	3	3
EGTA	—	—	—	1	1
BAPTA	—	—	1	—	—
Arginine-glutamate	—	—	120	—	—
Choline-Cl	—	—	—	—	120

Compositions of each solution. The pH was adjusted to 7.6 with TMA-OH in the truncation internal and Ca^{2+} clamp solutions and with Na-OH in the other solutions. The osmolarity was 245 in the truncation dialysis solution and 260 in all others. The free Ca^{2+} concentration in the truncation dialysis solution was 500–600 nM unless otherwise noted.

One set of experiments (those of Fig. 16) required a complete change of the nucleotide concentrations within the outer segment during the flash response. This was difficult at room temperature, as the time required for diffusion into the outer segment was comparable to the duration of the flash response. At 5–8°C, however, the duration of the flash response was much longer than the diffusion time. Low temperatures were achieved by cooling the solutions entering the chamber with a Peltier device (Ferrotec America, Chelmsford, MA) and blowing cold, dry air from a vortex tube (Illinois Tool Works, Glenview, IL) over the chamber. The temperature near the outer segment was monitored with a small thermocouple (Harvard Apparatus, Holliston, MA). All solutions flowed continuously to ensure that the temperature was uniform and steady; solution changes were made with the pipes mounted on the piezoelectric translation stage as described above.

In some experiments changes in the outer segment's free internal Ca^{2+} concentration were suppressed by inhibiting Ca^{2+} influx and efflux. Ca^{2+} efflux was inhibited by removing internal K^+ or external Na^+, both of which are required for Na^+/K^+, Ca^{2+} exchange (Cervetto et al., 1989); Ca^{2+} influx was inhibited by lowering the external Ca^{2+} concentration to reduce or eliminate the driving force on Ca^{2+} ions. For truncated outer segments (Yau and Nakatani, 1985), K^+ was omitted from the dialyzing solution and the solution in the suction electrode; the free Ca^{2+} concentration was buffered to 500–600 nM in the dialyzing solution and to a few nM inside the suction electrode. For intact cells, the inner segment was held in the suction electrode while the outer segment was superfused with a solution lacking Na^+ and Mg^{2+} and containing 10–20 nM free Ca^{2+} (Nakatani and Yau, 1988a; Matthews et al., 1988). Under these conditions the dark current was carried by outward movement of K^+ and remained relatively stable (<10% change) for periods of 30–60 s, after which the outer segment was superfused with Ringer's for at least 30 s.

The experiment illustrated in Fig. 2 tested for residual light-induced changes in the free Ca^{2+} concentration in intact cells whose outer segments were superfused with a solution lacking Na^+ and containing low Ca^{2+}. Dim flash responses were recorded from an intact rod with the Ca^{2+} changing freely (*thin trace* in Fig. 2 *A*) or with changes in Ca^{2+} suppressed (*thin trace* in Fig. 2 *B*). The rod was then superfused for 15 min with a solution containing 10 μM BAPTA-AM, a membrane-permeable Ca^{2+} buffer. Responses to the flash were recorded again with the Ca^{2+} changing freely or held constant (*thick traces* in Fig. 2, *A* and *B*). Increasing the Ca^{2+} buffering capacity of the outer segment should slow changes in free Ca^{2+} and thus render Ca^{2+} feedback less effective in accelerating the flash response. Indeed, exposure to BAPTA slowed the control flash response

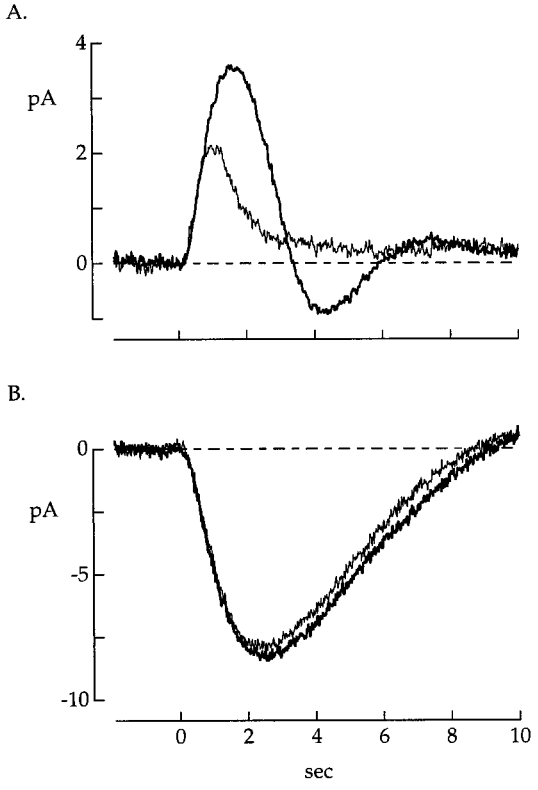

FIGURE 2 Test for residual light-induced changes in the internal Ca^{2+} concentration when the outer segment was superfused with a 0 Na^+, low Ca^{2+} solution (see Materials and Methods). Flash strength was 1.3 photons μm^{-2}. (*A*) Dim flash responses measured in an intact rod with the inner segment in the suction electrode and the outer segment superfused with Ringer's, allowing the Ca^{2+} concentration to change freely. The response shown by the thin trace was measured before exposure to BAPTA-AM; the response shown by the thick trace was measured after the cell was superfused with 10 μM BAPTA-AM for 15 min and returned to Ringer's. Increasing the Ca^{2+} buffering capacity of the outer segment by exposure to BAPTA-AM clearly altered the dim flash response. The dark current with the Ca^{2+} changing freely was -13 pA. (*B*) Dim flash responses measured from the same cell as in *A*, but with light-induced changes in the internal Ca^{2+} concentration suppressed by superfusing the outer segment with a solution lacking Na^+ and containing low Ca^{2+}. The response shown by the thin trace was measured before BAPTA exposure, the response shown by the thick trace after. The addition of Ca^{2+} buffer to the outer segment had only a small effect on the dim flash response, indicating that residual light-induced changes in Ca^{2+} were small on the time scale of the response. The dark current was $+16$ pA.

and made it biphasic (Fig. 2 *A*), as observed previously (Torre et al., 1986). If changes in the internal Ca^{2+} alter the flash response when the outer segment is superfused with the 0 Na^+, low Ca^{2+} solution, the addition of BAPTA would alter the flash response under these conditions as well. In this case, however, the flash response changed little (Fig. 2 *B*). In three experiments of this type, changes in the time to peak and amplitude after the addition of BAPTA were at least fivefold smaller with the Ca^{2+} held constant than with it changing freely. The relative insensitivity of the flash response to exogenous buffer indicates that superfusion with the 0 Na^+, low Ca^{2+} solution effectively suppressed light-induced changes in Ca^{2+} within the outer segment.

THEORY

This section presents a model that relates the statistics of rhodopsin shutoff to the time-dependent mean and variance of the elementary response. We use this model in two ways. In the Results, the calculated mean and variance are compared to the quantities measured when rhodopsin shutoff was slowed and presumably made more variable (see Figs. 12 and 17). In the Discussion, the model is used to explore how the low variability of the elementary response constrains possible mechanisms of reproducibility (Fig. 18). The parameters of the model were held fixed for all calculations, as the aim was to explore classes of models for reproducibility rather than to provide accurate fits to individual measurements.

Relation between rhodopsin activity and change in current

We begin by relating the time course of rhodopsin's catalytic activity to changes in PDE activity, cGMP concentration, and membrane current. The model for the transduction cascade is similar to that of Pugh and Lamb (1993) and Nikonov et al. (1998). A more complete description can be found in Rieke and Baylor (1996).

Active rhodopsin decreases the cGMP concentration by catalyzing the activation of transducin, which in turn activates a cGMP phosphodiesterase (PDE) (Fig. 1). As this latter step occurs quickly (reviewed by Pugh and Lamb, 1993), we ignore any delay introduced by transducin activation and approximate the time derivative of the PDE activity $P(t)$ as

$$\frac{dP(t)}{dt} = \sigma R(t) - \phi(P(t) - P_D), \quad (1)$$

where σR is the rate of PDE activation for a rhodopsin activity R, ϕ is the rate constant for PDE deactivation, and P_D is the dark PDE activity. Equation 1 describes the light-induced change in PDE activity as the output of a low-pass filter with time constant ϕ^{-1} applied to rhodopsin's catalytic activity.

The time derivative of the cGMP concentration $G(t)$ depends on the difference between the rates of cGMP synthesis and hydrolysis (Fig. 1),

$$\frac{dG(t)}{dt} = \gamma - P(t)G(t), \quad (2)$$

where γ is the rate of cGMP synthesis. Pugh and Lamb (1993) applied Eq. 2 at short times after a flash, assuming that the synthesis rate was constant, that the PDE activity could be approximated by a delayed ramp, and that $P(t) \gg P_D$. In this case the change in cGMP concentration is proportional to $\exp(-at^2)$, where a is a constant proportional to the flash strength. Their analysis accurately describes the initial rise of the flash response.

In intact rods, a light-induced fall in the free Ca^{2+} concentration affects several elements of the transduction cascade (reviewed by Koutalos and Yau, 1996). The most pronounced of these effects is an increase in the rate of cGMP synthesis and a consequent speeding of response

recovery, and for simplicity we will include only this effect of Ca^{2+} in the model. The free Ca^{2+} concentration depends on the rates of Ca^{2+} influx through the cGMP-gated channels and Ca^{2+} efflux by Na^+/K^+, Ca^{2+} exchange (Nakatani and Yau, 1988b; Cervetto et al., 1989). Although a complete description of the exchange rate requires several time constants (Rispoli et al., 1993; Gray-Keller and Detwiler, 1994; McCarthy et al., 1996; Murnick and Lamb, 1996), the fastest component should dominate during the flash response. Thus the time derivative of the free Ca^{2+} concentration C can be approximated by

$$\frac{dC(t)}{dt} = qI(t) - \beta C(t), \tag{3}$$

where q is a constant relating changes in the free Ca^{2+} concentration to the membrane current I (Nakatani and Yau, 1988b), and β is the rate constant for Ca^{2+} efflux. β depends on the activity of both the exchange proteins and intracellular Ca^{2+} buffers. The dependence of the rate of cGMP synthesis on the free Ca^{2+} concentration can be described by the Hill curve (Koch and Stryer, 1988; Koutalos et al., 1995a):

$$\begin{aligned}\gamma &= \frac{\gamma_{max}}{1 + (C/K_{GC})^m} \\ &\approx \frac{\gamma_{max} K_{GC}^m}{C^m},\end{aligned} \tag{4}$$

where γ_{max} is the maximum synthesis rate, K_{GC} and m are affinity and cooperativity constants, and the approximation is valid for $C \gg K_{GC}$. This approximation should hold for small changes in the current, as the free Ca^{2+} concentration in darkness is two to three times greater than K_{GC}.

We write the change in cGMP concentration as $g(t) = G(t) - G_D$, where G_D is the dark cGMP concentration. $g(t)$ can be approximated from Eqs. 1–5 as a filtered version of the rhodopsin activity $R(t)$, assuming that the changes in the PDE activity, cGMP concentration, and free Ca^{2+} concentration are small relative to the dark values (see Rieke and Baylor, 1996):

$$g(t) \approx \int_0^t F(\tau)R(t-\tau)d\tau. \tag{5}$$

When the free Ca^{2+} concentration and hence the synthesis rate γ are constant, the Fourier transform of the filter F is given by

$$\tilde{F}(\omega) = -\frac{\sigma G_D}{(\phi - i\omega)(P_D - i\omega)}, \tag{6}$$

where $\omega = 2\pi f$ is the angular frequency in radians per second and $\tilde{F}(\omega) = \int \exp(i\omega t)F(t)dt$. When the Ca^{2+} concentration changes freely, the Fourier transform of the filter takes the form

$$\tilde{F}(\omega) = -\frac{\sigma G_D}{(\phi - i\omega)}\left[P_D + \frac{3m\beta^2 P_D}{\beta^2 + \omega^2} - i\omega + \frac{3mi\omega\beta P_D}{\beta^2 + \omega^2}\right]^{-1}. \tag{7}$$

The changes in cGMP concentration described by Eqs. 5–7 depend on two time scales: 1) that for the decay of the light-activated PDE activity, determined by the time course of rhodopsin's catalytic activity and the decay rate ϕ of PDE; and 2) that for the restoration of the cGMP concentration, determined by the dark cGMP synthesis rate (equal to $P_D G_D$) and the rate constant β for the fall in Ca^{2+}. For all calculations we assumed $m = 2$, $P_D = 0.1\ s^{-1}$, $\phi = 2\ s^{-1}$, and $\beta = 2\ s^{-1}$ (see Koutalos et al., 1995a,b; Rieke and Baylor, 1996).

Equation 5 describes the change in the internal cGMP concentration produced by rhodopsin activity. The membrane current rapidly tracks this change (Karpen et al., 1988), and for cGMP concentrations at which less than half the channels are open, the current can be approximated as (Zimmerman and Baylor, 1986)

$$I \approx kG^3, \tag{8}$$

where $k \approx 8 \times 10^{-3}$ pA/μM^3 in toad rods (Rieke and Baylor, 1996). The approximation in Eq. 8 should be valid for the experiments described here; in intact cells ~5% of the channels were open in the dark, whereas in experiments on truncated outer segments 10–20% of the channels were open in darkness. Assuming $g(t) \ll G_D$, Eq. 8 can be expanded and approximated by the linear term. The result is that the change in current $i(t)$ is approximately

$$\begin{aligned}i(t) &= I_D - I(t) \\ &\approx -3kG_D^2 g(t).\end{aligned} \tag{9}$$

Equation 9 should provide a good description of the single photon current response, as the change in cGMP is thought to be small compared to the dark value at all points along the outer segment (Pugh and Lamb, 1993). Equations 5 and 9 can be combined to estimate the current change produced by rhodopsin activity $R(t)$,

$$i(t) \approx -3kG_D^2 \int_0^t F(\tau)R(t-\tau)d\tau, \tag{10}$$

where the Fourier transform of the filter $F(\tau)$ is given by Eq. 6 or 7.

The model described above treats the cGMP and Ca^{2+} concentrations as spatially homogeneous, ignoring diffusion. If the current change in an intact rod is linearly related to rhodopsin activity, then the time course and amplitude of the current response depend only on the total changes in cGMP and Ca^{2+} and not on their spatial extent. In this case diffusion can be ignored. In truncated outer segments, diffusion causes the cGMP concentration to depend on longitudinal position, and in outer segments without cGMP syn-

thesis, diffusion restores the cGMP concentration and dark current. To test the effect of diffusion on the single photon response in truncated outer segments with cGMP synthesis proceeding normally, we compared the behavior of the model described above with that of a model including cGMP diffusion (see Rieke and Baylor, 1996). Calculated flash responses with and without diffusion were nearly identical, and thus for simplicity we neglected diffusion. Dim flash responses in truncated outer segments without cGMP synthesis were fitted assuming that restoration of the cGMP concentration by diffusion occurred at a constant rate γ_{eff}. This simplified treatment again provided calculated responses in close agreement with those calculated when diffusion was included.

Stochastic model for rhodopsin shutoff

Equation 10 provides an estimate of the elementary current response given the time course of the activity of a single photoisomerized rhodopsin molecule. Intertrial fluctuations in the response could arise either from variations in the time course of rhodopsin's activity or from fluctuations in the transduction cascade. Because a single active rhodopsin rapidly generates hundreds or thousands of active transducin molecules (reviewed by Pugh and Lamb, 1993), stochastic fluctuations in the transducin activity or transducin's activation products should be small compared to fluctuations in the rhodopsin activity. In this case the filter F is effectively deterministic, and variability in the elementary response can be attributed to rhodopsin. To investigate how the measured response fluctuations constrain fluctuations in the rhodopsin activity, we considered two stochastic models for rhodopsin shutoff. In each model the time course of the catalytic activity of a single rhodopsin molecule was calculated and the corresponding elementary response was generated from Eq. 10, which assumes that the cascade responds linearly and deterministically to rhodopsin activity. This procedure was repeated for several hundred trials, and the time-dependent ensemble mean and variance were calculated and compared with experiment (Fig. 18).

The effect of feedback control of rhodopsin shutoff on the mean and variance of the elementary response was investigated assuming that the putative feedback signal accumulated linearly with time and accelerated rhodopsin shutoff with a cooperativity h. Thus the feedback caused the probability density for rhodopsin shutoff to increase proportionally with t^h, where t is the time after photoisomerization. Shutoff was assumed to occur as a single step.

The effect of multiple transitions in rhodopsin shutoff on the mean and variance of the elementary response was investigated assuming that each transition was memoryless and first-order. Transitions were assumed to occur sequentially with rate constants proportional to the catalytic activity of the state preceding the transition; thus states with low catalytic activity decayed more slowly than states with high activity. This choice of rate constants and activities was made for two reasons. First, this model distributes rhodopsin's cumulative activity equally among the states and produces the maximum reduction in the variance of the elementary response for a given number of states. Second, a gradual decline in rhodopsin activity is consistent with the approximately exponential time course of rhodopsin's activity measured in Fig. 7.

RESULTS

Reproducibility of the single photon response

Variability in the amplitude and time course of the elementary response constrains the mechanisms responsible for reproducibility. Thus we analyzed the statistics of the responses to a fixed dim flash, producing an average of less than one photoisomerization per trial; a short section of one such experiment is shown in Fig. 3 *A*. Each flash generated zero, one, or two photoisomerizations and a quantized change in current. The intertrial variability in the response is consistent with the Poisson statistics that govern the probability of photoisomerization (Baylor et al., 1979b; see below). Each elementary response had a similar amplitude and shape. This reproducibility allows responses to zero, one, or two photoisomerizations to be clearly distinguished, as shown in Fig. 3 *B*, where 50 individual responses are superimposed. The largest response presumably resulted from two or three photoisomerizations. Thus the rod is an accurate photon counter that reliably detects a single photoisomerization and differentiates between one and two photoisomerizations.

Variability of the response amplitude and time course

The accuracy with which the number and timing of photoisomerizations can be deduced from the rod current is limited by cellular dark noise and variability in the elementary response. We investigated the fluctuations in the elementary response itself by separating them from dark noise, which consists of continuous baseline fluctuations and occasional discrete events caused by the thermal activation of rhodopsin (Baylor et al., 1980). Discrete events were identified as those occurring at times unrelated to the flash (*arrows* in Fig. 3 *A*); trials containing a discrete event were removed before the statistics of the remaining responses were analyzed. Elementary response fluctuations were separated from continuous dark noise by comparing responses to zero and one photoisomerization, as described below.

Fig. 4 *A* shows a histogram of the response amplitudes, measured as the difference between the mean current in a 0.5 s interval before the flash and a similar interval centered on the maximum of the average response (shown in *inset*). The peaks in the histogram correspond, respectively, to zero, one, and two photoisomerizations. Amplitude histograms were fitted assuming that responses to individual photoisomerizations were additive, that the number of photoisomerizations produced by repeated flashes obeyed Pois-

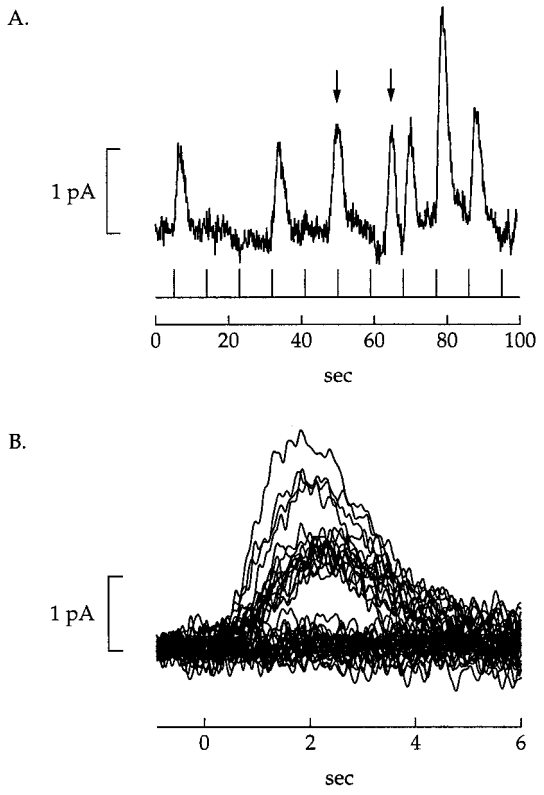

FIGURE 3 Single photon responses. (*A*) Photocurrents from an intact rod stimulated by a series of dim flashes delivered at the times indicated by the flash monitor. The flashes produced an average of 0.7 photoisomerizations per trial. Two events from spontaneous rhodopsin isomerization are marked by arrows. The outer segment was in the suction electrode, and the cell was superfused with a bicarbonate-based Ringer's. Flash stimuli were applied over a transverse slit 10 μm wide positioned near the middle of the outer segment. Bandwidth: 0–3 Hz. The dark current was −25 pA. (*B*) Superimposed responses to 50 flashes, including those in *A*. The responses were recorded sequentially, except for the removal of responses clearly contaminated by thermal events (such as those marked by *arrows* in *A*). The mean current in a 1 s interval before the flash has been set to zero in each case to correct for baseline drift and to facilitate comparison of the response shapes. Responses to zero, one, and two photoisomerizations can be clearly distinguished, as each elementary response had an amplitude and time course similar to those of the others. The largest response presumably resulted from two or three photoisomerizations.

son statistics, and that the noise in darkness and in the elementary response amplitude were independent and additive with Gaussian amplitude distributions. The expected number of responses with an amplitude between A and $A + \Delta A$ is

$$N(A) = N_{tot}\Delta A \sum_{n=0}^{\infty} \frac{\exp(-\bar{n})\bar{n}^n}{n!} [2\pi(\sigma_D^2 + n\sigma_A^2)]^{-1/2} \times \exp\left(-\frac{(A - n\hat{A})^2}{2(\sigma_D^2 + n\sigma_A^2)}\right), \quad (11)$$

where N_{tot} is the total number of responses, $\hat{A}$ is the mean amplitude of the elementary response, $\bar{n}$ is the mean number of photoisomerizations per flash, σ_D^2 is the variance of the current amplitude in darkness, and σ_A^2 is the variance in the elementary response amplitude. The first term in the sum is the probability that the flash produced n photoisomerizations, and the remaining terms give the probability that the response to n photoisomerizations had an amplitude A. The smooth curve in Fig. 4 *A* was drawn according to Eq. 11, with $N_{tot} = 410$, $\hat{A} = 0.66$ pA, $\bar{n} = 0.67$, $\sigma_D = 0.09$ pA, and $\sigma_A = 0.14$ pA. The ratio of the mean amplitude $\hat{A}$ to its standard deviation σ_A provides a measure of the reproducibility of the elementary response amplitude. In 13 cells $\hat{A}/\sigma_A$ was 4.6 ± 0.9 (mean ± SD). In five additional cells, σ_A was less than σ_D and could not be accurately estimated; in each of these cells $\hat{A}/\sigma_A$ was greater than 5. Thus the mean amplitude of the elementary response was about five times larger than its standard deviation, in agreement with previous measurements (Baylor et al., 1979b; Schnapf, 1983).

The entire shape of the elementary response was also nearly constant across trials, as revealed by the following analysis. Responses to single photoisomerizations ("singles") were separated from responses to zero ("failures") or multiple photoisomerizations. For example, in Fig. 4 *A* responses with amplitudes between 0.3 and 1.0 pA were taken as singles. Each of these responses was fitted by the equation for the impulse response of a cascade of m identical and independent first-order low-pass filters,

$$i_{fit}(t) = a(t/\tau)^{m-1}\exp(-t/\tau), \quad (12)$$

where a is a scaling factor for the response amplitude and τ is the time constant of each filter. Fitting was done by choosing the values of a and τ that minimized the mean square error between $i_{fit}(t)$ and $i(t)$ for each response $i(t)$ while holding m fixed at 4. A histogram of the values of τ for the cell of Fig. 4 *A* is shown in Fig. 4 *B*. The dark noise contributed little to the width of the distribution, as judged by adding a fixed elementary response to each failure (responses with amplitudes less than 0.3 pA in Fig. 4 *A*) and fitting the resulting ensemble as before. The smooth curve in Fig. 4 *B* is a Gaussian with a mean $\bar{\tau} = 0.58$ s and standard deviation $\sigma_\tau = 0.12$ s. The ratio $\bar{\tau}/\sigma_\tau$ provides a measure of the reproducibility of the shape of the elementary response. In 11 cells $\bar{\tau}/\sigma_\tau$ was 4.8 ± 1.0 (mean ± SD). Thus both the mean amplitude and temporal width of the elementary response were about five times larger than their respective standard deviations. This degree of constancy provides a constraint for evaluating possible mechanisms for reproducibility.

Time-dependent variance of the elementary response

The low variability of the elementary response was verified by comparing the time-dependent variance of responses to a fixed dim flash with the square of the mean response. If the elementary response has a stereotyped waveform $f(t)$ and the average number of isomerizations per flash is $\bar{n}$, then the mean response is $\bar{n}f(t)$ and the variance due to Poisson

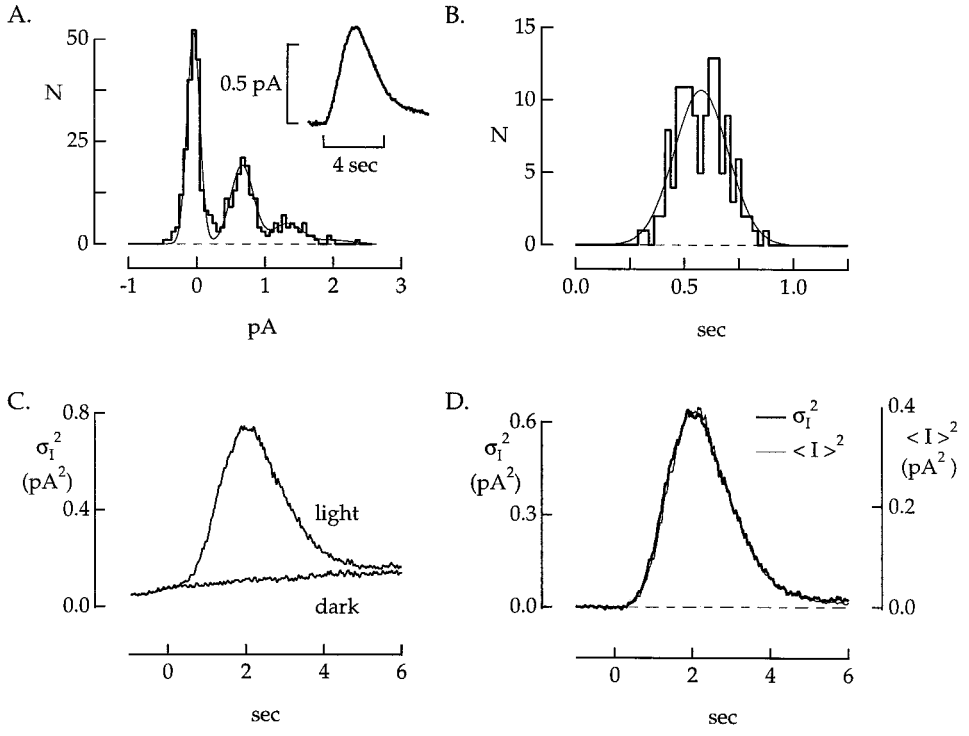

FIGURE 4 Reproducibility of the single photon response. Recordings were made from an intact rod superfused with bicarbonate-based Ringer's with its outer segment in the suction electrode. Flash stimuli were applied over a transverse slit 10 μm wide positioned near the middle of the outer segment. The dark current was −23 pA. (*A*) Amplitude histogram constructed from a series of 410 dim flash responses like those in Fig. 3. The inset shows the mean response; the flash was delivered at the beginning of the horizontal scale bar. The amplitude of each response was measured as the average decrease in current between 1.75 and 2.25 s. The smooth curve fitted to the experimental histogram was calculated according to Eq. 11, which assumes that the noise in darkness and the noise in the elementary response amplitude are independent and additive and that the number of photoisomerizations per flash is described by Poisson statistics. The fit was calculated for 0.67 photoisomerizations per flash, a mean elementary response amplitude of 0.66 pA, a standard deviation of the current in darkness of 0.09 pA, and a standard deviation of the elementary response amplitude of 0.14 pA. (*B*) Histogram measuring reproducibility of the elementary response shape (stepped curve) constructed from the 129 responses from *A*, with an amplitude between 0.3 and 1.0 pA. Each response was fitted according to Eq. 12 with the output of a cascade of four identical, independent low-pass filters. The free variable in the fit was the low-pass filter time constant, and these time constants form the histogram plotted. The smooth curve is a Gaussian with a mean of 0.58 s and a standard deviation of 0.12 s. (*C*) Time-dependent variance of responses measured in darkness ("dark") and in the presence of the flash stimulus ("light"). The variance measured in darkness resulted from baseline drift and instrumental and cellular noise. The additional variance with light exposure arose from intertrial variability in the measured responses; this variance contains contributions from Poisson fluctuations in the number of photons absorbed per flash and variability in the elementary response. Same experiment as in *A* and *B*. (*D*) Light-dependent variance increase (*thick trace*) and square of the mean response (*thin trace*). The variance increase is the difference (light − dark) between the two traces in *C*. As described in the text, the variance increase would have the same shape as the square of the mean response if each photoisomerization produced an identical response and the variance increase were solely attributable to variations in the number of photoisomerizations. Significant fluctuations in the shape of the elementary response would cause the variance to have a shape different from that of the square of the mean. The scaling factor between the variance and the square of the mean indicated that the flash produced an average of 0.61 photoisomerizations.

fluctuations in the number of photoisomerizations is $\bar{n}f^2(t)$. Thus for an elementary response of fixed size and shape, the time-dependent variance is proportional to the square of the mean, and the constant of proportionality is the average number of photoisomerizations per flash. Fig. 4 *C* shows the variance for all of the responses contributing to the histogram in Fig. 4 *A* as well as the variance in darkness, which resulted from baseline drift, cellular dark noise, and instrumental noise. Assuming that the light-induced variance and the variance in darkness are independent and additive, the difference (light − dark) is the variance attributable to the flash response itself. This difference had the shape of the square of the mean response (Fig. 4 *D*). The scaling factor gave an average of 0.61 photoisomerizations per flash, which is comparable to the estimate of 0.67 obtained by fitting the amplitude histogram of Fig. 4 *A*. In 11 of 16 cells the square of the mean response had the same shape as the variance increase. In the other five cells the variance during the response recovery was slightly greater than the square of the mean. In all cases fluctuations in the shape of the elementary response contributed much less to the variance than did Poisson fluctuations in the number of photoisomerizations.

What is the intrinsic time-dependent variance of the elementary response, separated from variance introduced by fluctuations in the number of photoisomerizations? This residual variability is generated by the phototransduction process and should further constrain the mechanism that

confers reproducibility. Elementary responses were isolated by the method used in constructing Fig. 4 *B*. Fig. 5 *A* shows the time-dependent variance of the elementary response and the variance in darkness from one such experiment. Precautions were taken to avoid systematic changes in the elementary response during the course of the experiment, as these would inflate the residual variance (see Materials and Methods). Fig. 5 *B* shows the variance increase attributable to the elementary response and, for comparison, the square of the mean response (note different axis scales). The small residual variance of the elementary response is an upper limit to the intertrial variability of the signal triggered by a single photoisomerized rhodopsin. It appears to consist of two components, one reaching its maximum near the peak of the response and the other during the recovery phase. The relative magnitudes of these components differed from cell to cell. To pool measurements from multiple cells, the time and amplitude axes were normalized by the time to peak and square of the peak amplitude of the mean response; the normalized variance and mean response squared were then averaged (Fig. 5 *C*, 12 cells). The variance was 15–20 times smaller than the square of the mean response until well after the peak of the response. The Discussion explores the implications of this small residual variability for possible mechanisms of reproducibility.

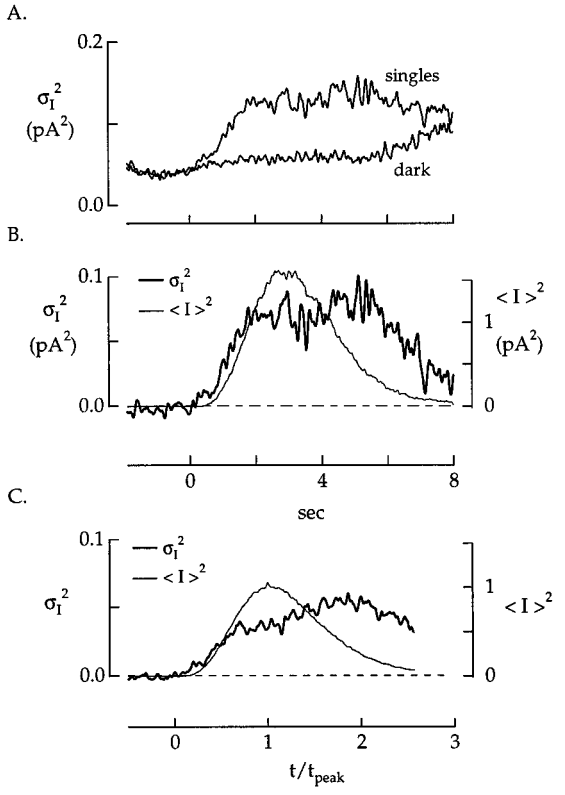

FIGURE 5 Residual variability of the single photon response. (*A*) Time-dependent variance of 71 elementary responses ("singles") and 119 traces recorded in darkness ("dark"). Elementary responses were identified from a histogram of the response amplitudes as described in the text. Responses clearly contaminated by discrete noise events were excluded. The variance measured in darkness was caused by instrumental and cellular dark noise. The additional variance of the singles is due to intertrial variability in the elementary response. Current was collected from only the distal third of the outer segment to reduce the cellular dark noise. Light stimuli were applied over a 10 μm wide slit centered on the region from which current was collected. The flash produced an average of 0.56 photoisomerizations. (*B*) Variance of the elementary response from *A* (*thick trace*) and square of the mean response (*thin trace*). Assuming that the variance of the singles and the dark variance were independent and additive, the variance in the elementary response could be isolated as the difference (singles − dark). Note that the peak of the variance is ~15 times smaller than the square of the mean. (*C*) Collected results from experiments on 12 cells. In each cell the variance and the square of the mean elementary response were measured as in *A* and *B*. Each measure was normalized by the time to peak and the square of the peak amplitude of the mean elementary response. The average of the normalized variance and square of the mean response are plotted. Note that the variance is ~15 times smaller than the square of the mean.

Time course of rhodopsin's catalytic activity

Experiments such as those in Figs. 3–5 quantify the reproducibility of the rod's elementary response. Before exploring possible mechanisms for reproducibility, we examined a general problem that bears upon all potential mechanisms: the time course of rhodopsin's catalytic activity. It has been suggested that rhodopsin deactivation dominates the rate of decline in PDE activity after a flash (Pepperberg et al., 1994; Corson et al., 1994) and, alternatively, that rhodopsin activity decays more quickly (Murnick and Lamb, 1996; Sagoo and Lagnado, 1997; Nikonov et al., 1998). The essential question for reproducibility is whether the amplitude alone or both the amplitude and the shape of the elementary response are sensitive to fluctuations in rhodopsin's catalytic activity. If the catalytic activity is confined to a brief time interval at the beginning of the response, variability in rhodopsin's activity should affect the response amplitude but not its shape. If, instead, the catalytic activity persists through a significant fraction of the elementary response, variability in the activity should affect both the response amplitude and shape. The experiments described below indicate that rhodopsin's activity persists through a significant fraction of the dim flash response in truncated outer segments at constant internal Ca^{2+}. We use this result in subsequent experiments to test the mechanisms responsible for reproducibility.

Time course of rhodopsin activity in truncated outer segments

The average time course of rhodopsin's catalytic activity was measured in truncated outer segments by abruptly increasing the gain of transducin activation by rhodopsin at specific times after a flash. The method for changing the gain is shown schematically in Fig. 6. Photoisomerized rhodopsin binds transducin-GDP and the GDP dissociates. The rhodopsin-transducin complex can then bind either GTP or GDP, but only GTP binding produces activated transducin. Thus transducin was activated with high gain when the solution dialyzing the outer segment contained 1

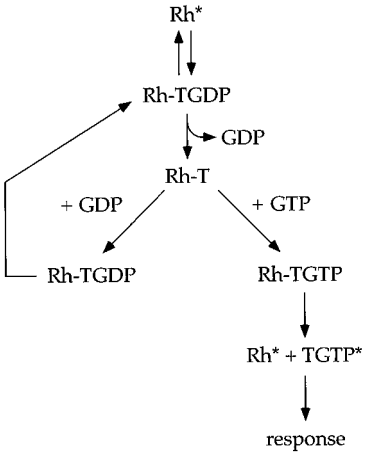

FIGURE 6 Procedure for changing rhodopsin-transducin gain. Photoisomerization promotes the binding of transducin-GDP to isomerized rhodopsin and the dissociation of GDP. This leaves the nucleotide binding site on transducin empty. Binding of GTP causes dissociation of rhodopsin-transducin and transducin activation. Binding of GDP simply returns rhodopsin-transducin to the initial state, from which rhodopsin and transducin-GDP or GDP alone can dissociate. Thus a high GDP concentration causes several futile cycles of GDP binding and unbinding for each transducin that is activated. A high GTP concentration suppresses futile cycling and causes efficient transducin activation. This procedure allows the gain of transducin activation to be lowered without using a very low GTP concentration, which alone could slow rhodopsin phosphorylation or arrestin binding and thus prolong the flash response (see Fig. 13). This procedure assumes that increasing the GTP concentration does not cause significant GDP-GTP exchange on the α subunit of transducin; biochemical experiments (Fung, 1983) support this assumption.

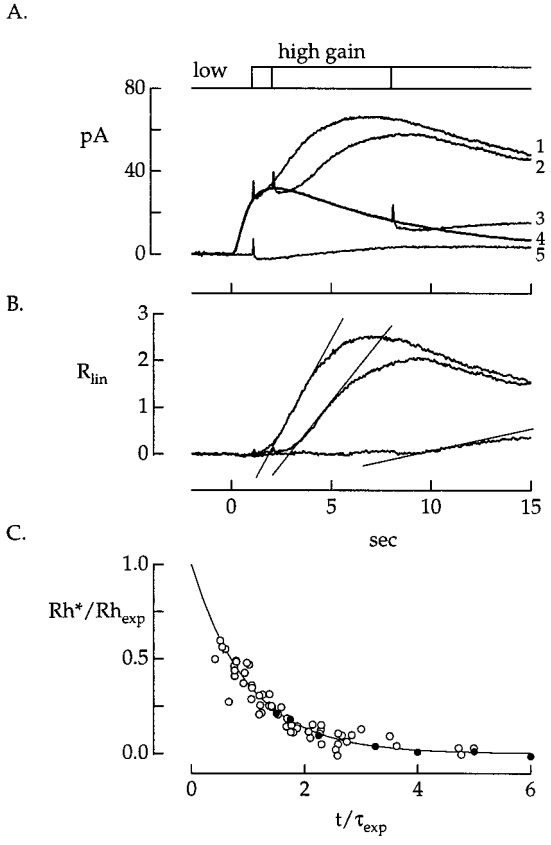

FIGURE 7 Time course of rhodopsin's catalytic activity measured by abruptly increasing the gain of transducin activation. (*A*) Original records from one such experiment. The outer segment was initially dialyzed with a solution containing 10 μM GTP and 90 μM GDP, giving low rhodopsin-transducin gain. At a specific time after a flash was delivered, the dialyzing solution was switched to one containing 1 mM GTP and 90 μM GDP, giving high rhodopsin-transducin gain. In traces 1–3 this solution change was made 1, 2, and 8 s after the flash, as shown in the upper timing trace. Trace 4 is a flash response measured in the low-gain dialyzing solution. Trace 5 is the change in current produced by the solution change in the absence of a flash. Flash stimuli were applied over a 10 μm wide transverse slit and produced ~60 photoisomerizations. The dark current was −75 pA. (*B*) Linearized difference currents from *A*. Each of the responses in *A* was linearized (see text) to yield a proportional measure of rhodopsin activity. The two corrected control responses—the flash in the low gain solution (*trace 4*) and the current change produced by the solution change alone (*trace 5*)—were subtracted from the corrected responses to both the flash and solution change (*traces 1–3*). The initial slope of these corrected difference currents is proportional to rhodopsin's catalytic activity. (*C*) Collected results from 13 experiments. Results from each experiment have been normalized by the amplitude Rh_{exp} and time constant τ_{exp} of the best fit exponential, $Rh(t) = Rh_{exp}\exp(-t/\tau_{exp})$. The mean time constant was 2.3 ± 0.2 s (mean ± SEM). Measurements from the experiment in *A* and *B* are plotted as filled circles.

mM GTP and 90 μM GDP and with low gain when the dialyzing solution contained 10 μM GTP and 90 μM GDP. The addition of GDP to compete with GTP allowed the gain to be lowered without using an extremely low GTP concentration, which in the absence of GDP might slow rhodopsin shutoff (see Fig. 6 legend).

Fig. 7 shows results from one GTP-jump experiment. Initially the outer segment was dialyzed with the low-gain solution. A flash producing ~10 photoisomerizations was delivered, and the dialyzing solution was switched to the high-gain solution after a delay indicated in the upper trace. Responses with solution changes initiated 1, 2, and 8 s after the flash are superimposed in Fig. 7 *A* (*traces 1–3*). Two control responses were also recorded: a flash response with the low-gain dialyzing solution (*trace 4*) and a response to the solution change alone to check for cGMP synthesis at the high GTP concentration (*trace 5*). As described below, rhodopsin's catalytic activity was estimated by linearizing each response and isolating the change in current produced by the increase in rhodopsin's ability to activate transducin.

We estimated rhodopsin's catalytic activity from records such as those in Fig. 7 *A* by correcting for the nonlinear relations between the current and cGMP concentration and between the rate of change in cGMP concentration and rhodopsin activity. From Eqs. 2 and 8 the time derivative of the inward current, dI/dt, is related to the rates of cGMP synthesis and hydrolysis by

$$\frac{dI}{dt} = \frac{dI}{dG}\frac{dG}{dt} = 3I[\gamma_{eff}/G - P_D - p_F] - 3p_S I, \quad (13)$$

where G is the cGMP concentration, γ_{eff} is the rate of cGMP diffusion into the outer segment from the dialyzing solution,

P_D is the dark PDE activity, p_F is the light-evoked increase in PDE activity in the low-gain dialyzing solution, and p_S is the increment in PDE activity due to residual rhodopsin activity at the time of the solution change. The additional change in current 0.5–1 s after the solution change was relatively small and approximated a perturbation superimposed on the flash response. In this case the first term on the right side of Eq. 13 describes the current change produced by the flash response in the absence of the solution change, and the second term describes the additional change produced by increasing the rate of transducin activation. Thus the increment in PDE activity p_S produced by the solution change is proportional to $(\mathrm{d} \ln I/\mathrm{d}t)_S$, the contribution of the solution change to the slope of the logarithm of the current. As p_S varies linearly with the rhodopsin activity at a fixed time after the solution change (see Eq. 1), the rhodopsin activity is also proportional to $(\mathrm{d} \ln I/\mathrm{d}t)_S$. Each measured trace was corrected by computing the logarithm of the inward current at each instant of time; the two linearized control traces were then subtracted from the linearized trace with the solution change. The initial slope of the corrected difference current measures rhodopsin's catalytic activity (Fig. 7 *B*). The slope was measured in a 0.25–0.5 s time window starting 0.25 s after the solution change. This analysis was repeated for several delays between the flash and solution change.

Rhodopsin activities $Rh^*(t)$ measured in different outer segments were normalized by the amplitude Rh_{exp} and time constant τ_{exp} of the best-fit exponential $Rh_{exp}\exp(-t/\tau_{exp})$, where t is the time between the flash and the slope measurement. Results from 13 experiments are collected in Fig. 7 *C*. The average rhodopsin activity declined approximately exponentially over the range of times probed with a time constant of 2.3 ± 0.2 s (mean ± SEM). The time constant measured when the flash suppressed less than 30% of the dark current was similar to that when a brighter flash was used (2.1 s versus 2.5 s); thus the correction for the nonlinear relation between current and rhodopsin activity described above did not significantly influence τ_{exp}. From these experiments we conclude that rhodopsin's catalytic activity in truncated outer segments declines on average with a time constant of 2–2.5 s. This relatively slow deactivation indicates that both the amplitude and shape of the elementary response should be sensitive to fluctuations in rhodopsin's activity.

Further evidence that rhodopsin's catalytic activity was relatively long-lived in truncated outer segments came from experiments in which phosphorylation was slowed by lowering the ATP concentration. If rhodopsin deactivated quickly, a slight prolongation of its activity would increase the amplitude of the dim flash response but would have relatively little effect on the time to peak. If rhodopsin's activity persisted through a significant fraction of the response, prolongation should have similar effects on the amplitude and time to peak. In seven outer segments in which dim flash responses were measured at 200 and 20 μM ATP (e.g., Fig. 12), the time to peak increased by 30 ± 4% in low ATP, whereas the peak amplitude increased by 30 ± 8% (mean ± SEM). Thus the time to peak and peak amplitude of the elementary response were equally sensitive to slowing the time course of rhodopsin's catalytic activity, in agreement with the relatively slow deactivation profile measured in Fig. 7.

Comparison of deactivation kinetics in truncated and intact cells

A potential problem in the experiments described above is a slowing of rhodopsin shutoff due to diffusional loss of rhodopsin kinase or arrestin from the truncated outer segment. Three observations suggest that this was not significant during the 15–20 min period in which measurements were made. First, experiments described below indicate that neither phosphorylation nor arrestin binding dominated the time required for rhodopsin shutoff in truncated outer segments (Figs. 14 and 15). Second, the kinetics of dim flash responses measured in truncated outer segments with active cGMP synthesis were similar to those measured in intact cells at constant internal Ca^{2+} (see Materials and Methods): the time to peak and integration time were 3.6 ± 0.5 s and 7.9 ± 1.7 s in truncated outer segments and 4.4 ± 0.9 s and 7.1 ± 1.3 s in intact cells at constant internal Ca^{2+} (mean ± SD, 11 truncated outer segments, 11 intact cells). Third, the 2.3 s time constant for the decline of rhodopsin's catalytic activity in truncated outer segments is similar to that of 2–2.5 s measured for the decline in PDE activity in intact cells after saturating flashes (Pepperberg et al., 1994; Corson et al., 1994; Lyubarsky et al., 1996; Murnick and Lamb, 1996) and estimated after a dim flash (below).

To estimate the rate of PDE shutoff in intact cells after a dim flash, we analyzed the kinetics of responses measured with the outer segment Ca^{2+} concentration held constant (see also Lyubarsky et al., 1996; Nikonov et al., 1998). From Eq. 2 the PDE activity during the flash response can be estimated from the cGMP concentration $G(t)$, the basal PDE activity P_D, and dark cGMP concentration G_D as

$$P(t) = \frac{P_D G_D - \mathrm{d}G(t)/\mathrm{d}t}{G(t)}. \qquad (14)$$

where at constant internal Ca^{2+} the synthesis rate has been written as $\gamma = P_D G_D$. Equation 14 neglects the effect of spatial inhomogeneities in the cGMP concentration, a valid approximation provided the change in current is related linearly to the change in cGMP. $G(t)$ was estimated, using Eq. 9, from the average of 20–40 responses to a flash producing less than five photoisomerizations. The time course of the PDE activity was estimated from Eq. 14, assuming $P_D = 0.1\ s^{-1}$ (Rieke and Baylor, 1996). Fig. 8 illustrates this analysis. Fig. 8 *A* shows the average dim flash response of an intact cell with the internal Ca^{2+} held constant, and Fig. 8 *B* shows the time course of the PDE activity calculated from this flash response. The light-activated PDE activity in this cell declined with a time constant of 2.1 s (*smooth curve* in Fig. 8 *B*); in 11 cells the time constant was 2.6 ± 0.3 s (mean ± SEM). Thus after a dim flash, the PDE activity in an intact rod at constant Ca^{2+} declined at a rate similar to that of the decline

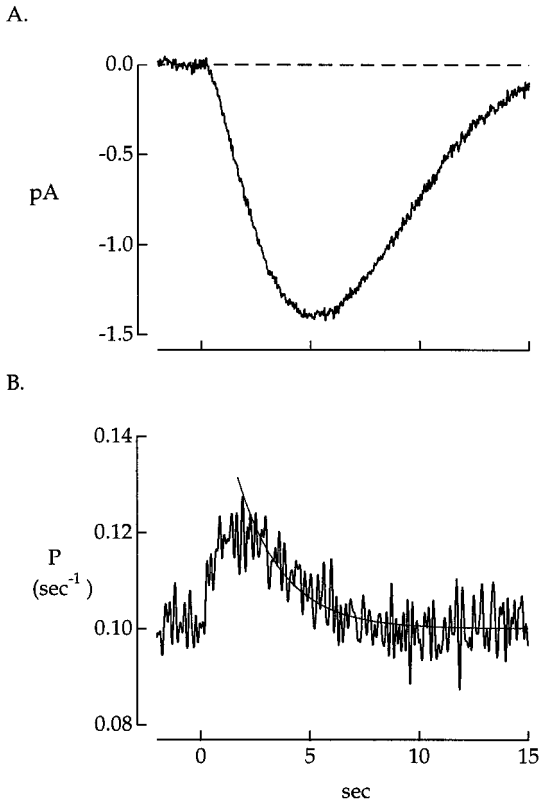

FIGURE 8 Time course of PDE activity after a dim flash. (*A*) Average dim flash response in an intact cell measured at constant internal Ca^{2+} (see Materials and Methods). The flash produced an average of 1.2 photoisomerizations. The dark current was +9.5 pA. (*B*) Time course of PDE activity calculated according to Eq. 14 from the flash response in *A*, assuming a mean dark PDE activity of 0.1 s^{-1}. The smooth curve is an exponential with a time constant of 2.1 s fitted to the measured trace between 3 and 15 s.

in rhodopsin activity in a truncated outer segment. This suggests that rhodopsin's activity is relatively long-lived in both truncated outer segments and intact cells at constant internal Ca^{2+}.

Summary

The general conclusion from the experiments in this section is that rhodopsin's catalytic activity in truncated outer segments at constant Ca^{2+} persists through a significant fraction of the elementary response. Thus both the amplitude and shape of the response should be sensitive to fluctuations in rhodopsin's activity. Below we use the sensitivity of the response shape to fluctuations in rhodopsin's activity to test the mechanisms that might mediate reproducibility.

Possible mechanisms for reproducibility

Experiments such as those illustrated in Figs. 3–5 indicate that the entire waveform of the elementary response is reproducible. This is unexpected because the response originates from a single rhodopsin molecule whose active lifetime might be expected to fluctuate from trial to trial (see Introduction). Rhodopsin shutoff is thought to result from one or two phosphorylations followed by arrestin binding (Ohguro et al., 1995). If the time required for phosphorylation or arrestin binding were the dominant delay in rhodopsin deactivation, the distribution of catalytic lifetimes would be approximately exponential. If the amplitude of the photocurrent were proportional to rhodopsin's catalytic lifetime, the distribution of photocurrent amplitudes would also be nearly exponential. For the exponential distribution, the ratio of the mean $\hat{A}$ to the standard deviation σ_A is 1, substantially less than the measured ratio of 5. The ratio $\hat{A}/\sigma_A$ would increase only slightly (as the square root of the number of steps) if rhodopsin shutoff involved two or three steps with similar rate constants, and the increase in $\hat{A}/\sigma_A$ would be less if the rate constants differed significantly. How, then, is such good reproducibility achieved? We tested the three possibilities outlined below.

Feedback control of single photon responses

An amplified product of photoisomerized, catalytically active rhodopsin could accumulate during the elementary response and act as a feedback signal that causes the response to terminate reproducibly. Such a feedback could reduce variability by regulating rhodopsin deactivation, or it could suppress the effects of variability in rhodopsin deactivation by acting at a later stage in the transduction cascade (Fig. 9 *A*). Several feedback pathways have been proposed to operate in phototransduction: acceleration of transducin shutoff by a reduction in the cGMP concentration (Arshavsky et al., 1992); acceleration of the rate of cGMP synthesis by the light-induced fall in Ca^{2+} (Koch and Stryer, 1988); and acceleration of rhodopsin shutoff by the fall in Ca^{2+} (Kawamura, 1993; Erickson et al., 1998) or by depletion of unactivated transducin near the active rhodopsin (Langlois et al., 1996).

Saturation

Saturation (Fig. 9 *B*) could reduce variability in the elementary response by making the photocurrent insensitive to intertrial fluctuations in rhodopsin's catalytic activity. For example, saturation might involve depletion of unactivated PDE on a single outer segment disk or closure of most or all of the cGMP-gated channels near the site of photon absorption.

Multiple steps in rhodopsin shutoff

Multiple steps in rhodopsin shutoff (Fig. 9 *C*) could cause the catalytic activity of each photoisomerized rhodopsin molecule to decline along a similar time course, leading to a reproducible elementary response. Fig. 9 *C* depicts each step as lowering rhodopsin's activity. This gradual decrease in the catalytic activity of a single molecule is consistent with the exponential decay of the average activity (Fig. 7).

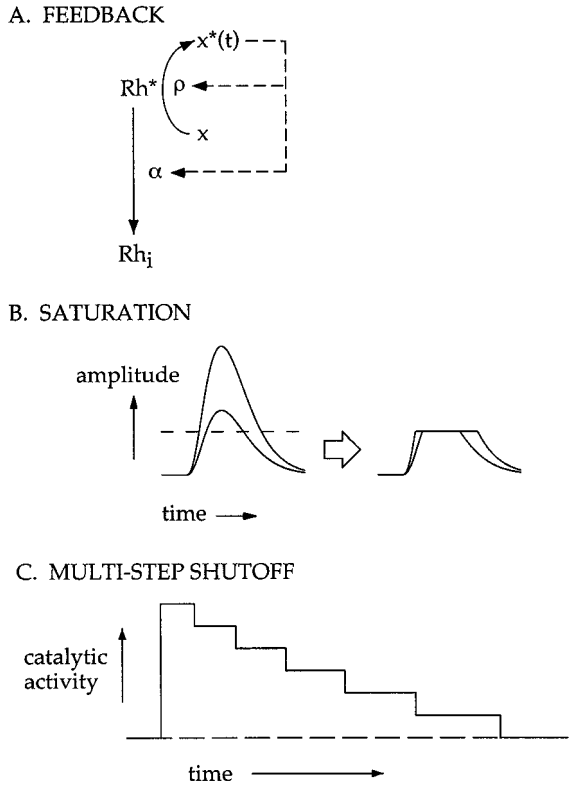

FIGURE 9 Possible mechanisms for reproducibility. The low variability of the elementary response indicates either low intertrial variability in rhodopsin's catalytic activity or suppression of the effects of such variability by the transduction cascade. Three potential mechanisms are shown schematically. (*A*) A feedback signal $x^*(t)$ might control the rate α of rhodopsin shutoff or the rate ρ of activation of a downstream product of rhodopsin. Feedback control of rhodopsin shutoff could reduce intertrial variability in rhodopsin's activity, whereas feedback to a downstream element of the cascade could make the membrane current insensitive to variability in rhodopsin's activity. (*B*) A saturation might cause the membrane current to be insensitive to variability in rhodopsin's activity. A saturation acting at the peak of the response such as that depicted here (e.g., local depletion of open cGMP-gated channels) could reduce variability in the response amplitude. (*C*) Rhodopsin's catalytic activity might deactivate through a series of transitions, each of which reduces the activity by a small amount and occurs after a stochastic, first-order delay. Despite variations in the timing of individual transitions, variability in rhodopsin's cumulative activity could be reduced.

Shutoff through a series of n steps, each terminated by a first-order transition, would reduce variability in rhodopsin's activity by at most by $1/\sqrt{n}$. The measured reproducibility would thus require about 25 steps, far more than can be accounted for by the two known steps in rhodopsin shutoff—phosphorylation and arrestin binding (Lagnado and Baylor, 1992).

Test of molecular mechanisms for reproducibility

Feedback

Ca^{2+} feedback. A light-induced fall in the free Ca^{2+} concentration regulates several elements of the transduction cascade (reviewed by Koutalos and Yau, 1996). Suppressing the fall in Ca^{2+} slows the dim flash response and increases its amplitude (Matthews et al., 1988; Nakatani and Yau, 1988a). The best documented consequence of the fall in Ca^{2+} is an increase in the rate of cGMP synthesis by guanylate cyclase (Koch and Stryer, 1988), but Ca^{2+} feedback can also act on the time course (Kawamura, 1993; Erickson et al., 1998; Sagoo and Lagnado, 1997) and the gain (Lagnado and Baylor, 1994; Murnick and Lamb, 1996) of rhodopsin's catalytic activity. Does Ca^{2+} feedback make the elementary response reproducible?

We tested for such a role of Ca^{2+} feedback by comparing dim flash responses from intact cells with the internal Ca^{2+} concentration held constant or freely changing (see Materials and Methods). The single photon response slowed and increased in amplitude when light-induced changes in internal Ca^{2+} were suppressed (Fig. 10 *A*). Nevertheless, responses to zero, one, and two photoisomerizations had distinguishable amplitudes (Fig. 10 *B*). In four cells enough responses were collected at constant internal Ca^{2+} to construct amplitude histograms; in these cells the ratio of the elementary response amplitude $\hat{A}$ to its standard deviation σ_A was 5 ± 2 (mean $\pm$ SD), not significantly different from the ratio when the Ca^{2+} changed freely. Further evidence for low variability of the elementary response at constant Ca^{2+} came from comparing the time-dependent variance increase to the square of the mean response. In all nine cells tested, Poisson fluctuations in the number of photons absorbed dominated the variance. In four of nine cells, the shape of the variance increase was similar to the square of the mean response. In the other five cells there was additional variance during the later part of the response (e.g., Fig. 10 *C*); this additional variance in the elementary response could have arisen from genuine variability in the elementary response or from intertrial variability in the procedure used to suppress changes in Ca^{2+}. In all nine experiments the scaling factor between the variance increase and the square of the mean response differed by $<20\%$ between runs with the internal Ca^{2+} held constant and with the Ca^{2+} changing freely. These results indicate that reproducibility was substantially maintained without Ca^{2+} feedback.

Analysis of responses at constant Ca^{2+} in truncated outer segments pointed to the same conclusion. Here it was not possible to collect enough responses for an amplitude histogram, and instead the time-dependent variance increase and the square of the mean response were compared. As in intact cells, the variance increase and square of the mean had similar shapes (e.g., see Fig. 17 *A*), indicating that the time course of the elementary response was reproducible.

Experiments such as those in Figs. 10 and 17 indicate that Ca^{2+} feedback speeds the recovery of the response but is not required for reproducibility.

Feedback pathways not based on Ca^{2+}. We tested for a larger class of feedback signals that might control rhodopsin shutoff, using the strategy shown schematically in Fig. 11 *A*. If the deactivation of rhodopsin's catalytic activity is regulated by a feedback signal $x(t)$ originating at or downstream

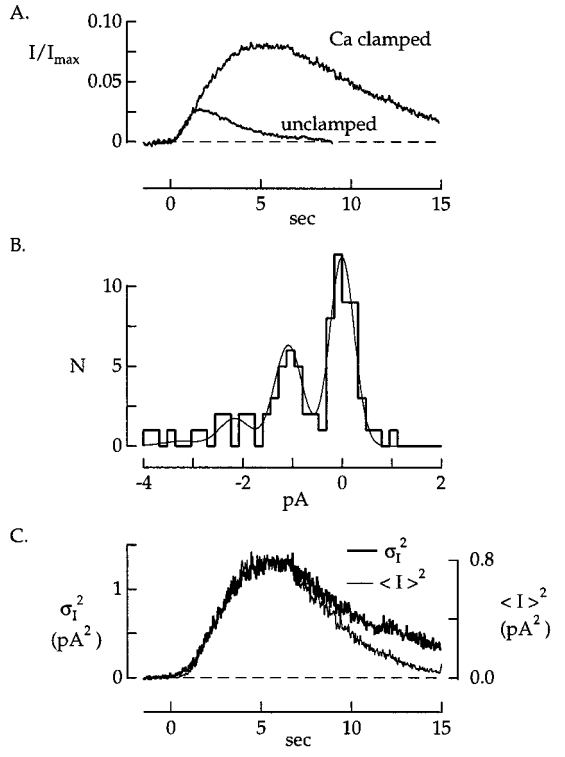

FIGURE 10 Single photon responses at constant internal Ca^{2+}. (*A*) Comparison of average dim flash responses measured with the Ca^{2+} allowed to change normally and with the Ca^{2+} held constant near its normal concentration in darkness (see Materials and Methods). Responses have been normalized by the dark current, which was −26 pA with the Ca^{2+} changing freely and +10 pA with the Ca^{2+} held constant. The flash produced an average of 0.6 photoisomerizations. (*B*) Amplitude histogram from 83 dim flash responses measured at constant internal Ca^{2+}. The amplitudes are negative because responses were inverted when the outer segment was superfused with the 0 Na^+, low Ca^{2+} solution (see Materials and Methods). Peaks corresponding to 0 and 1 photoisomerization can be clearly distinguished. The smooth curve was calculated according to Eq. 11 with $\hat{A} = -1.1$ pA, $\sigma_A = 0.25$ pA, $\sigma_D = 0.14$ pA, and $\bar{n} = 0.61$ photoisomerizations per flash. The mean response is shown in *A*. (*C*) Time-dependent variance increase (*thick trace*) and square of the mean response (*thin trace*) for responses contributing to the amplitude histogram in *B*. The light-dependent variance increase has been isolated by subtracting the variance measured in darkness from that measured from the flash responses, as in Fig. 4 *C*. The scaling factor between the variance and the square of the mean indicated an average of 0.59 photoisomerizations per flash.

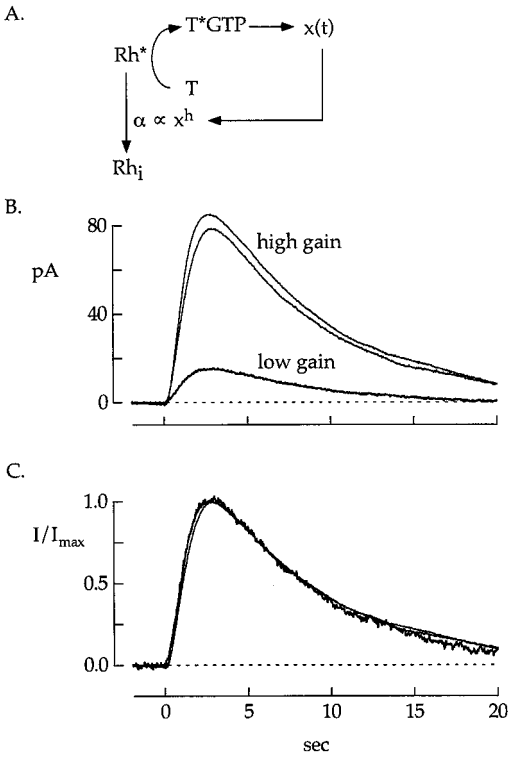

FIGURE 11 Test for feedback control of rhodopsin shutoff. (*A*) Experimental rationale. If rhodopsin shutoff is controlled by feedback from an activation product x of transducin, then lowering the rate of transducin activation should slow the accumulation of x and thus slow rhodopsin shutoff. As the shape of the dim flash response is sensitive to the time course of rhodopsin's activity, the presence of such a feedback should cause the shapes of dim flash responses at high and low rates of transducin activation to differ. (*B*) Dim flash responses measured in a truncated outer segment dialyzed with 90 μM GDP and 10 μM GTP, producing low rhodopsin-transducin gain (*thick trace*), or 90 μM GTP and 10 μM GDP, producing high gain (*thin traces*). The dialyzing solution contained 500 μM ATP in both cases. The response at low gain was measured between the two at high gain. This manipulation changed the rate of transducin activation by a factor of 5, as judged by the slope of the rising phase of the flash response. The dark current was −160 pA. Flash stimuli producing ~15 photoisomerizations were applied over a 10 μm wide transverse slit. (*C*) Responses at low and high gain from *B* scaled by their respective peak amplitudes. Despite the different rates of transducin activation, the response kinetics were not measurably different. This relative insensitivity of the response kinetics to changes in the rate of transducin activation indicates that rhodopsin's catalytic lifetime is not regulated by a feedback originating at or downstream of active transducin.

from active transducin, then the rate at which the feedback signal accumulates will be altered when the rhodopsin-transducin gain is changed. Slowing the accumulation of the feedback signal should delay the feedback effect and prolong rhodopsin's catalytic activity. Because rhodopsin deactivates relatively slowly (Fig. 7), prolonging rhodopsin's activity should prolong the dim flash response. The internal Ca^{2+} was held constant in these experiments (see Materials and Methods) to eliminate Ca^{2+} feedback.

The rhodopsin-transducin gain was altered by changing the GTP/GDP ratio (see Fig. 6). The high-gain dialyzing solution contained 90 μM GTP and 10 μM GDP, and the low-gain solution contained 90 μM GDP and 10 μM GTP. Changing the gain reversibly altered the amplitude of the dim flash response (Fig. 11 *B*) but did not change the response shape, as demonstrated by scaling each response by its peak amplitude (Fig. 11 *C*). A similar invariance of the response kinetics to a change in the rhodopsin-transducin gain was observed in each of five experiments. The gain, as judged by the initial rate of rise of the flash response, changed on average by a factor of 4.5 (range 3.1–6.1), whereas the time to peak changed by less than 5% in each experiment. These results indicate that rhodopsin deactivation is not under feedback control by transducin or any of its activation products, and therefore that such a feedback does

not explain the reproducibility of the elementary response. Ca^{2+} is excluded from this argument, as its internal concentration was held constant in these experiments.

Summary. The conclusion from this section is that reproducibility is not mediated by Ca^{2+} feedback to any element of the cascade (Figs. 10 and 17), nor is it mediated by any other feedback signal that controls rhodopsin shutoff and originates at or after active transducin (Fig. 11). In the Discussion we return to other potential feedback pathways that might contribute to reproducibility.

Saturation

A saturation—e.g., activation of all the PDE on a single outer segment disk or closure of all of the channels in a local region of the outer segment membrane—might make the elementary response reproducible by rendering the membrane current insensitive to variations in the time course of rhodopsin's catalytic activity. Such a saturation would manifest itself as a time-dependent nonlinearity, causing the current to become relatively independent of rhodopsin's activity. Several manipulations are known to increase the elementary response amplitude, including holding the internal Ca^{2+} constant (Matthews et al., 1988; Nakatani and Yau, 1988a; Fig. 10 *A*) and slowing or disabling rhodopsin phosphorylation (Palczewski et al., 1992; Chen et al., 1995); these observations indicate that complete saturation does not occur. The experiments presented below provide evidence against partial saturation as an explanation for reproducibility.

We compared the change in the dim flash response in truncated outer segments upon prolonging rhodopsin's activity with the change expected if the cascade responded linearly to rhodopsin activity—i.e., without saturation. Rhodopsin shutoff was slowed by lowering the ATP concentration in the dialyzing solution from 200 μM to 20 μM to slow rhodopsin phosphorylation. This manipulation increased the amplitude and slowed the kinetics of the dim flash response (Fig. 12 *A*). To determine whether lowering the ATP concentration indeed slowed rhodopsin shutoff, rhodopsin's catalytic activity was measured by the procedure in Fig. 7 5 s after a flash was delivered at high and low ATP; the activity in 20 μM ATP was about twice that in 200 μM ATP (two cells, data not shown). Fig. 12 *B* shows the expected effect of prolonging rhodopsin shutoff on the dim flash response, calculated using the linear model described in Eqs. 6 and 10. Rhodopsin's catalytic activity was assumed to decline exponentially with a time constant of 2.5 s at high ATP and 5 s at low ATP. The measured and calculated dim flash responses exhibited similar changes in amplitude and time to peak, indicating that significant saturation did not occur.

Further evidence that saturation cannot explain reproducibility is provided by the low variability of the response shape in both intact cells and truncated outer segments (see Figs. 4 *D*, 5 *C*, and 17 *A*). The relatively long duration of rhodopsin's catalytic activity in truncated cells at constant

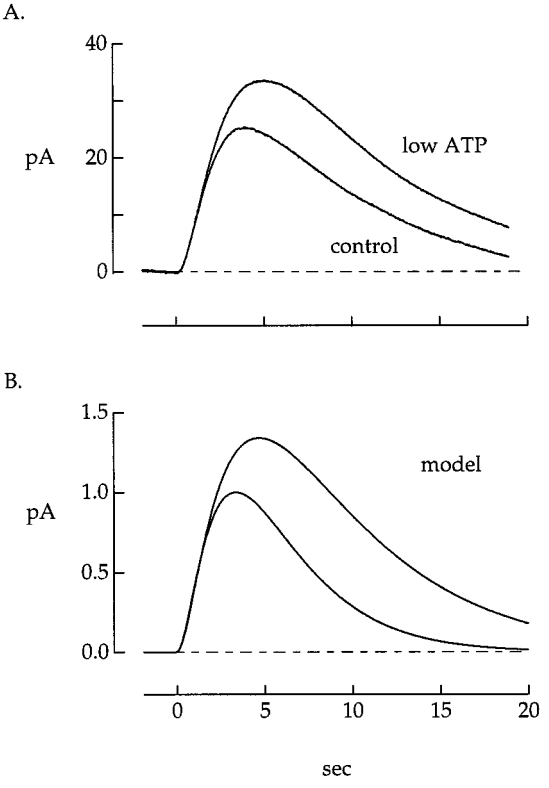

FIGURE 12 Test for saturation of the elementary response in a truncated outer segment. (*A*) Lowering the ATP concentration slowed and increased the amplitude of the dim flash response. The traces show average dim flash responses measured in a truncated outer segment dialyzed with a solution containing 1 mM GTP, 300 nM free Ca^{2+}, and either 200 μM ATP (*control*) or 20 μM ATP (*low ATP*). The dark current was -140 pA, and the flash produced an average of six to seven photoisomerizations. (*B*) Predicted change in flash response from the linear model described in Eqs. 6 and 10, assuming a basal PDE activity of 0.1 s^{-1} and an exponential decay of rhodopsin's catalytic activity, with a time constant of 2.5 s at high ATP and 5 s at low ATP.

internal Ca^{2+} (Fig. 7) indicates that the shape of the response should be sensitive to fluctuations in the time course of rhodopsin shutoff. A simple amplitude saturation should reduce variability only at the peak of the response; other types of saturation would similarly be expected to affect only part of the response.

Although these experiments do not rule out the possibility that saturation contributes to reproducibility, they show that saturation alone cannot account for it.

Multistep rhodopsin shutoff

Deactivation through a series of states, each terminated by a stochastic transition, could reduce intertrial variability in rhodopsin's catalytic activity (Fig. 9 *C*). To minimize variability, the product of the average activity and mean duration should be equal for each state, so that each controls the same fraction of rhodopsin's cumulative activity. If one state dominated, rhodopsin shutoff would effectively be controlled by a single transition and would exhibit large

intertrial variability. This model makes two testable predictions: 1) the known transitions in rhodopsin shutoff—phosphorylation and arrestin binding—cannot control a large fraction of rhodopsin's cumulative activity; and 2) variability in the elementary response should increase if a single transition is slowed so that the preceding state accounts for much of rhodopsin's cumulative activity.

Contributions of phosphorylation and arrestin binding. The known transitions in the shutoff of rhodopsin's catalytic activity are the binding of rhodopsin kinase, incorporation of a phosphate in rhodopsin's C terminus by the kinase, and the binding of arrestin. We will refer to kinase binding and the subsequent incorporation of a phosphate as phosphorylation. Several studies indicate that phosphorylation initiates response recovery (Nakatani and Yau, 1988c; Chen et al., 1995). Indeed, dim flash responses in truncated outer segments dialyzed with a solution lacking ATP rose to a plateau that was maintained for at least 30 s (four experiments; data not shown). Similarly, arrestin binding provides complete deactivation of rhodopsin's catalytic activity (Bennett and Sitaramayya, 1988; Xu et al., 1997). Experiments described below indicate that these requisite first and last steps in rhodopsin deactivation control only a small part of the integrated activity.

Kinase, arrestin, and transducin bind competitively to rhodopsin (Miller and Dratz, 1984; Krupnick et al., 1997). Thus while rhodopsin is bound to transducin it cannot be phosphorylated, nor can arrestin bind. The dissociation rate of rhodopsin-transducin, and hence the fraction of time rhodopsin is available for phosphorylation and arrestin binding, depend on the GTP concentration (Fig. 13); if the GTP concentration is sufficiently low, rhodopsin spends most of its time bound to transducin. This slowing in the dissociation rate of rhodopsin-transducin lowers the rate of transducin activation and thus the slope of the rising phase of the flash response, while at the same time decreasing the accessibility of rhodopsin for kinase and arrestin binding. If phosphorylation or arrestin binding controls most of rhodopsin's cumulative activity, lowering the GTP would slow rhodopsin shutoff and increase the time to peak of the response.

Fig. 14 *A* shows dim flash responses measured in a truncated outer segment dialyzed with 500 μM ATP and 10 or 4 μM GTP, concentrations low enough to prevent significant cGMP synthesis (Lagnado and Baylor, 1994; Rieke and Baylor, 1996). Lowering the GTP concentration from 10 to 4 μM decreased the response amplitude but did not change the time to peak, as shown in Fig. 14 *B*, where the responses are scaled by their peak amplitudes. Thus the rate of transducin activation, and hence the rates of phosphorylation and arrestin binding, can be decreased significantly, apparently without changing the rate of rhodopsin shutoff. In the same outer segment, use of a dialyzing solution containing 20 μM ATP provided a check that lengthening the lifetime of the rhodopsin-transducin complex slowed phosphorylation. Lowering the ATP concentration from 500 to 20 μM slowed the flash response, indicating that at low ATP phosphorylation controlled a significant fraction of rhodopsin's cumulative activity (see also Fig. 12). Under these conditions, lowering the GTP concentration changed both the rising phase and time to peak of the flash response (Fig. 14, *C* and *D*). In five similar experiments, reducing the GTP concentration from 10 to 4–5 μM affected both the response amplitude and time to peak at low ATP, but only the amplitude at high ATP.

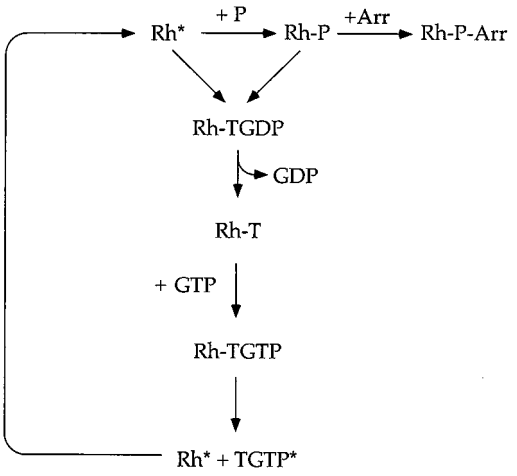

FIGURE 13 Procedure for testing the contributions of kinase and arrestin binding to the time course of rhodopsin shutoff. Rhodopsin kinase and arrestin compete with transducin for a single binding site on rhodopsin. Thus while rhodopsin is bound to transducin, it is not accessible to the kinase or arrestin. In the absence of GDP, the dissociation rate of rhodopsin-transducin is determined by the GTP concentration; lowering the GTP concentration slows dissociation of rhodopsin-transducin and thus slows the binding of kinase and arrestin. The rate of transducin activation, measured from the initial slope of the flash response, indicates how much kinase and arrestin binding have been slowed. This maneuver should slow the deactivation of rhodopsin's catalytic activity and the shape of the dim flash response if either the kinase or the arrestin binding rate limits rhodopsin shutoff.

To collect results from multiple experiments such as that in Fig. 14, each response was fitted using the model described by Eqs. 6 and 10. The fitted parameters were the initial rate of transducin activation σ and the rate of rhodopsin deactivation α, which were chosen to minimize the mean square error between the measured and calculated response; the other parameters of the model were held fixed at the values given in Theory. σ and α were normalized in each experiment by the values for the fit to the response measured at 10 μM GTP. Results from 18 outer segments dialyzed with 500 μM ATP are collected in Fig. 15, which plots the normalized rate of rhodopsin shutoff against the normalized rate of transducin activation. If phosphorylation or arrestin binding limited the time course of rhodopsin deactivation, lowering the rate of transducin activation by a factor of a would slow rhodopsin deactivation by the same factor, and the points would fall along the line of slope 1. The points fall above this line, indicating that the rate of rhodopsin deactivation was relatively insensitive to slowing phosphorylation and arrestin binding. Thus the experiments summarized in Fig. 15 indicate that the time required for phosphorylation and arrestin binding cannot account for the time course of rhodopsin's catalytic activity.

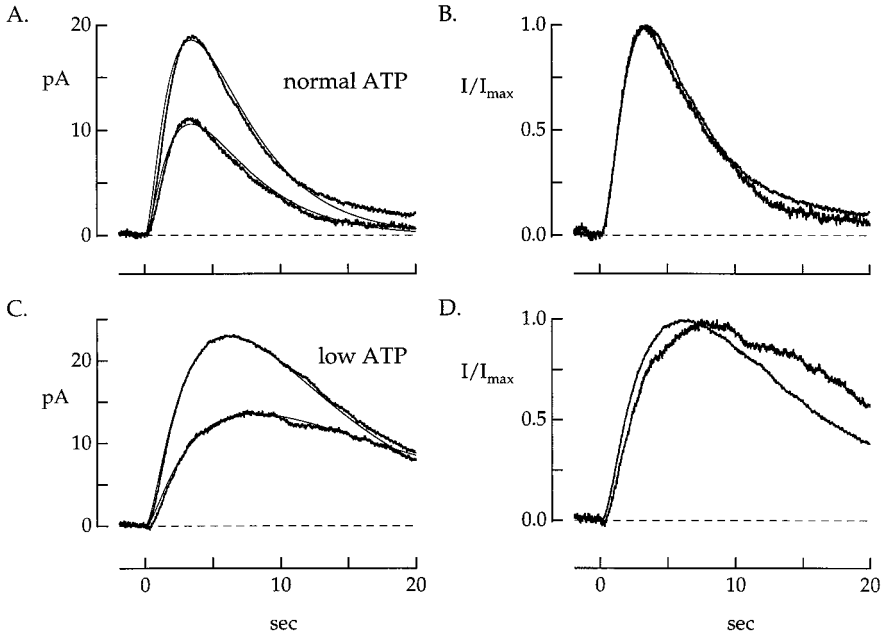

FIGURE 14 Time required for phosphorylation and arrestin binding failed to explain the time course of rhodopsin's catalytic activity. The dark current was 80 pA. Flash stimuli producing ~10 photoisomerizations were applied over a 10 μm wide transverse slit. (*A*) Averaged dim flash responses (10–15 trials) measured in a truncated outer segment dialyzed with 500 μM ATP and 10 or 4 μM GTP. Lowering the GTP concentration decreased the slope of the rising phase of the flash response, as expected for a decreased rate of transducin activation. The time to peak of the response, however, changed relatively little. The smooth traces were calculated according to Eqs. 6 and 10, assuming that rhodopsin's catalytic activity declined with an exponential time course. The fits were obtained by varying the rate constants for rhodopsin shutoff and transducin activation. Fits to the responses at high and low GTP were calculated using identical time constants for rhodopsin shutoff (2.1 s), whereas the rate of transducin activation was decreased by a factor of 1.8 at low GTP. (*B*) Responses from *A* scaled by their peak amplitudes to facilitate comparison of the response kinetics. (*C*) Control responses measured in the same outer segment. These responses, measured before those in *A*, were measured while the outer segment was dialyzed with 20 μM ATP and, again, either 10 or 4 μM GTP. Lowering the ATP slowed the flash response, presumably by slowing the rate of binding of kinase-ATP to active rhodopsin. In this case lowering the GTP concentration affected both the slope of the rising phase and the time to peak of the response. This result is expected if kinase binding is rate limiting at low ATP and stabilizing rhodopsin-transducin does indeed further slow kinase binding. Smooth traces fit to the measured responses were calculated as described in *A*, using a rhodopsin shutoff rate of 8.3 s at high GTP and 16.6 s at low GTP and a decrease in the rate of transducin activation by a factor of 2.1 at low GTP. (*D*) Scaled responses from *C*.

Phosphorylation accounts for a small fraction of rhodopsin deactivation. A second experiment tested the role of phosphorylation in rhodopsin shutoff. The timing of phosphorylation was controlled by removing ATP from a truncated outer segment to disable phosphorylation, delivering a flash, and then supplying ATP only during a brief time window near the peak of the response. Experiments were carried out at 5–8°C to slow the response relative to diffusion and allow effective removal of ATP during the flash response. Responses recovered fully when the outer segment was dialyzed with ATP for 10 s beginning at the time of the flash (Fig. 16 *A*, *thick trace*), recovery being identical to that when ATP was present throughout (Fig. 16 *A*, *thin trace*). Removal of ATP 10 s before a dim flash eliminated the response recovery (Fig. 16 *B*). As the response reached a peak in less than 10 s, ATP removal disabled phosphorylation in less than 20 s. Thus phosphorylation was restricted to a time window of at most 30 s after the flash in the experiment of Fig. 16 *A*, and much of the response recovery took place after phosphorylation had occurred. Similar results were observed in six outer segments.

The significance of these results for rhodopsin shutoff depends critically on whether rhodopsin's activity persists throughout the flash response at low temperatures or whether another process is responsible for the slow recovery. In particular, lowering the temperature could slow transducin's GTPase activity, causing it to limit the rate of PDE deactivation after a flash. A lower bound to the rate of PDE deactivation was obtained by delivering a flash in the absence of ATP, waiting for the response to reach a plateau, and then disabling transducin activation by removing GTP from the dialyzing solution. Upon removal of GTP, the dark current recovered with a time constant determined by the decay of activated PDE and the time required for GTP to diffuse from the outer segment. At 5–8°C recovery upon GTP removal was faster than the normal recovery of the flash response in the presence of ATP (exponential time constant of 27 $\pm$ 4 s versus 57 $\pm$ 9 s, mean $\pm$ SEM in six outer segments). Thus neither the time required for transducin and PDE shutoff nor that required for diffusion limited the response recovery, suggesting that rhodopsin continued to activate transducin throughout much of the response.

These results indicate that at low temperatures phosphorylation is a requisite step in the initiation of rhodopsin

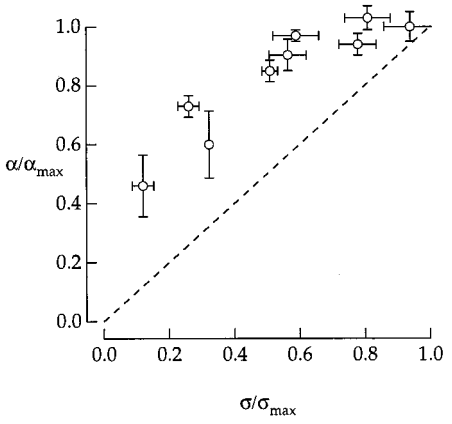

FIGURE 15 Collected results on the contributions of phosphorylation and arrestin binding to the time course of rhodopsin shutoff. The normalized rate of rhodopsin shutoff α is plotted against the rate of transducin activation σ from 18 experiments. Responses at GTP concentrations ranging from 0.5 to 10 μM were measured and fitted as in Fig. 14 to obtain estimates of the rate constants for rhodopsin shutoff and transducin activation. These rate constants were normalized by the estimates α_{max} and σ_{max} from responses at 10 μM GTP to compare responses across cells; each point represents the mean ± SD from at least three measurements. All of the points fall above the dashed line, which represents the expectation if the rate of rhodopsin shutoff and rate of transducin activation were equally sensitive to a change in the GTP concentration. The relative insensitivity of the rate of rhodopsin shutoff to changes in the GTP concentration indicates that the time course of rhodopsin shutoff is not limited by phosphorylation or arrestin binding.

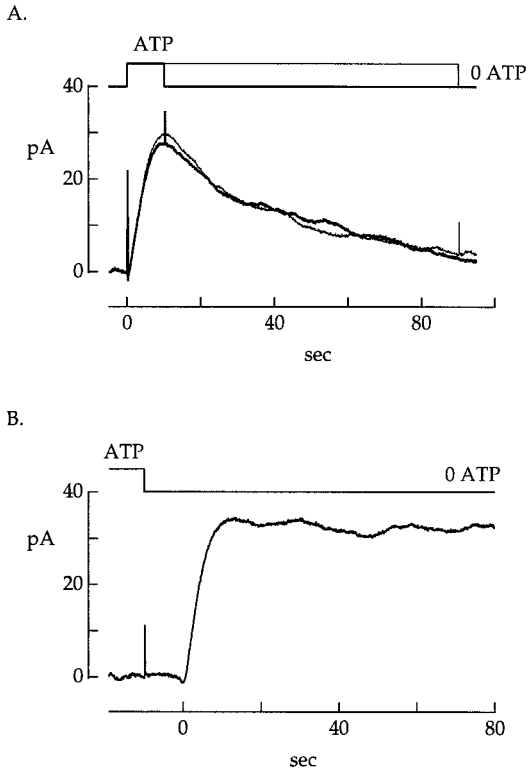

FIGURE 16 Contribution of phosphorylation to the shutoff of rhodopsin's catalytic activity. Dim flash responses were recorded from a truncated outer segment at 8°C dialyzed with a solution containing either 0 or 40 μM ATP. The timing of the changes in the dialyzing solution is given in the upper traces. The dark current was −75 pA. Flash stimuli producing ~80 photoisomerizations were applied over a 10 μm wide transverse slit. (*A*) Superimposed responses when the outer segment was dialyzed with ATP for 10 s or 90 s after the flash. The presence of ATP for a relatively brief time near the peak of the response was sufficient for a normal recovery. Thus phosphorylation was required for the initiation of recovery but did not itself much decrease rhodopsin's catalytic activity. (*B*) Response to a flash delivered 10 s after removal of ATP from the dialyzing solution. No recovery was evident, indicating that removal of ATP effectively suppressed phosphorylation and rhodopsin shutoff. As the response reached a peak in ~10 s, this indicates that effective ATP removal required 20 s at most.

shutoff, but itself controls only a small fraction of rhodopsin's integrated activity.

Increased variability when phosphorylation is rate limiting. A second prediction of the multistep model for rhodopsin deactivation is that variability in the elementary response should increase if one step in rhodopsin shutoff is made rate limiting. This prediction was tested by slowing rhodopsin phosphorylation and examining the time-dependent variance of the dim flash response. Interleaved groups of 5–10 dim flash responses at 200 and 20 μM ATP were recorded in a truncated outer segment, with a minimum of 20 responses recorded in each condition. Averaged responses at 200 and 20 μM ATP are shown in Fig. 12. At high ATP the light-dependent variance increase was well described by the square of the mean response (Fig. 17 *A*), consistent with a reproducible elementary response and Poisson fluctuations in the number of absorbed photons. At low ATP the variance increase was considerably larger (Fig. 17 *B*). A similar increase in variance at low ATP was observed in five experiments. In each experiment the increase in variance was comparable to the variance introduced by the Poisson statistics of photon absorption, and thus accurate photon counting was not possible at low ATP. The increased variance at low ATP can be explained if rhodopsin's activity became more variable when phosphorylation limited rhodopsin deactivation.

The increased variance at low ATP can be compared to that expected from a simple stochastic model of rhodopsin shutoff and the linear model for the transduction cascade described in Eqs. 6 and 10. Phosphorylation was assumed to act as a single-step process described by a time constant τ_P, and the remainder of rhodopsin shutoff was assumed to be deterministic. At low ATP, τ_P was assumed to account for half of the time course of rhodopsin shutoff. The average number of photoisomerizations was fixed by the measured scaling factor between the variance increase and square of the mean response. Fig. 12 shows the average flash responses calculated for these conditions. Fig. 17 *C* shows the calculated square of the mean response and time-dependent variance for a flash producing an average of seven photoisomerizations. The calculated increase in variance is similar to the measurements in Fig. 17 *B*. Thus variability of the elementary response increased by an amount consistent with the increase in rhodopsin's variability when its shutoff proceeded effectively as a one- or two-step process.

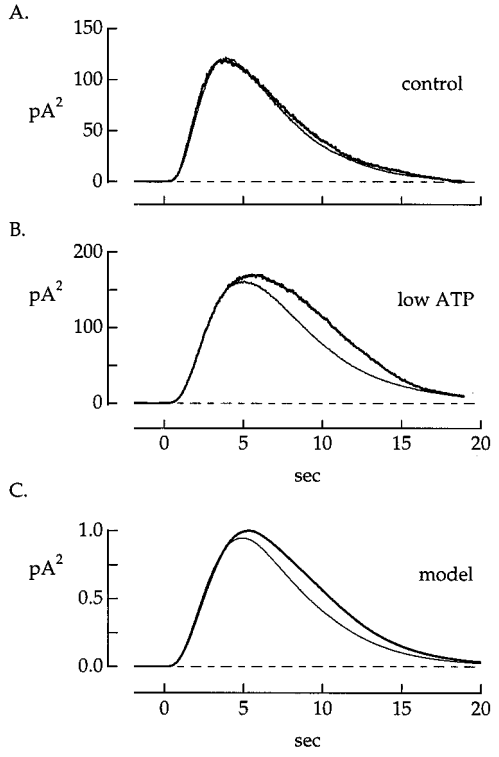

FIGURE 17 The elementary response variance increased when rhodopsin shutoff slowed. The dark current was −140 pA. Flash stimuli were applied over a 10 μm wide tranverse slit. (*A*) Time-dependent variance increase (*thick trace*) and square of mean response (*thin trace*) from 22 trials when the outer segment was dialyzed with 200 μM ATP and 1 mM GTP. The scaling factor between the variance and the square of the mean indicated an average of six photoisomerizations per trial. (*B*) Variance increase and square of mean from 29 trials when the outer segment was dialyzed with 20 μM ATP and 1 mM GTP. The scaling factor between the variance and the square of the mean indicated an average of seven photoisomerizations per trial. (*C*) Variance and square of the mean response calculated according to Eqs. 6 and 10, assuming that on average the time required for phosphorylation accounted for half of rhodopsin's cumulative activity. Phosphorylation was modeled as a memoryless, first-order transition with a time constant τ_P of 2.5 s. Rhodopsin deactivation after phosphorylation was assumed to follow a deterministic, exponential time course with a time constant of 2.5 s. The variance was calculated from 500 responses.

Summary. The relatively long time course of rhodopsin's catalytic activity (Fig. 7) and the inability of phosphorylation and arrestin binding to account for this time course (Figs. 14–16) indicate that additional steps contribute to rhodopsin deactivation. The increased variance in the elementary response when phosphorylation was rate limiting for rhodopsin shutoff (Fig. 17) indicates that the measured current was sensitive to variability in rhodopsin's activity. These results suggest that a reproducible deactivation process involving multiple transitions may occur between phosphorylation and arrestin binding.

DISCUSSION

Summary

We tested three possible mechanisms for the reproducibility of the rod's elementary response: 1) feedback to rhodopsin or a downstream element of the cascade; 2) saturation of an activation product of rhodopsin; and 3) multistep deactivation of rhodopsin. The results indicate that reproducibility is not explained by saturation, by Ca^{2+} feedback of any kind, or by control of rhodopsin shutoff by a feedback signal originating at or after active transducin. We did not directly test three possible mechanisms: 1) feedback from a signal other than Ca^{2+} to an activation product of rhodopsin; 2) feedback control of rhodopsin shutoff by a molecular species activated in parallel with transducin; and 3) decay of rhodopsin's catalytic activity through a series of steps. We now discuss each of these possibilities.

Feedback to cascade downstream of rhodopsin

A feedback acting downstream of rhodopsin from a signal other than Ca^{2+} could conceivably make the membrane current insensitive to variability in rhodopsin's catalytic activity. This seems unlikely, however, for several reasons. First, the low variability of the elementary response would require the feedback to be quite powerful. In the absence of phosphorylation the elementary response rises to a maintained plateau (Chen et al., 1995; Fig. 16), whereas a powerful feedback controlling amplification should cause at least some response recovery. Second, the increase in the mean and variance of the current when rhodopsin shutoff was slowed is consistent with calculations that assume that the membrane current is fully sensitive to variability in rhodopsin's activity (Fig. 17). Thus although feedback signals other than Ca^{2+} may control amplification, they probably do not mediate the reproducibility of the elementary response.

Feedback to rhodopsin originating before active transducin

Regulation of rhodopsin shutoff by feedback from a molecular species activated in parallel with transducin might conceivably explain reproducibility. Such a mechanism must meet two requirements to be effective: 1) the molecule mediating the feedback must accumulate rapidly, so that variability in the feedback signal itself is small; and 2) the rate of rhodopsin shutoff must be highly sensitive to the amplitude of the feedback signal. Even if the feedback signal were effectively deterministic, it would have to exert its effect on a single photoisomerized rhodopsin molecule, presumably by binding to it. Stochastic fluctuations in the binding reaction set a limit to the effectiveness of this mechanism, as shown in Fig. 18, which compares the calculated time-dependent variance of the elementary response with the measured variance from Fig. 5. The feedback signal was assumed to have negligible variability, to accumulate linearly with time after photoisomerization, and to act with a cooperativity h on the rate α of rhodopsin shutoff—i.e., $\alpha \propto t^h$. The time-dependent variance of the elementary response was calculated using the model described in Eqs. 7 and 10. Higher cooperativities caused the rhodopsin shutoff rate to increase more abruptly and thus were

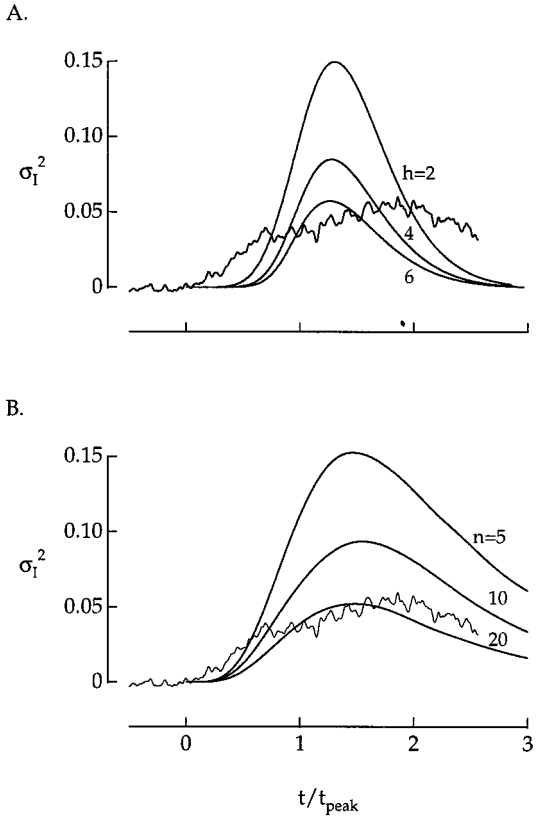

FIGURE 18 Constraints on models for reproducibility from variance of single photon response. (*A*) Feedback. Suppression of fluctuations in the elementary response by feedback control of rhodopsin shutoff depends on the cooperativity with which the feedback acts; feedback signals acting with high cooperativities cause rhodopsin to shut off abruptly and thus more effectively decrease response fluctuations. The cooperativity required to explain the measured reproducibility was explored by calculating the time-dependent variance of the elementary response for a stochastic model in which rhodopsin shutoff was controlled by a feedback signal x accumulating linearly with time and acting with a cooperativity h. Thus the rate of rhodopsin shutoff was $\alpha \propto x^h$. The variance is shown for $h = 2$, 4, and 6. The noisy trace is the measured time-dependent variance of the elementary response from Fig. 5. A cooperativity of 4–6 was required to explain the measured reproducibility. (*B*) Multistep shutoff. Rhodopsin shutoff through multiple stochastic transitions could reduce variability in the elementary response. The number of steps required was explored by calculating the time-dependent variance for a stochastic model in which rhodopsin's activity decays through n first-order transitions. The traces plotted are for $n = 5$, 10, and 20. Fifteen to twenty transitions were required to explain the measured reproducibility.

more effective in reducing the variance, although the abrupt shutoff of rhodopsin's activity produced by this model confined the variance to a much shorter time window than the measured variance. Reduction of the variance to measured levels required a cooperativity greater than 4.

The main argument against this mechanism is that there are no obvious candidates for the feedback signal. The experiments in Results indicate that the signal cannot be Ca^{2+}, nor can it originate at or downstream of active transducin. Furthermore, the experiment of Figs. 14 and 15 suggests that the molecular events controlling most of rhodopsin's cumulative activity are independent of transducin binding to rhodopsin, making rhodopsin kinase and arrestin unlikely feedback signals. Activated rhodopsin is not known to interact with any other molecular species.

Multistep shutoff of rhodopsin's catalytic activity

We believe that reduction in the intertrial variability of rhodopsin's catalytic activity by shutoff through a series of steps is the most likely explanation for reproducibility. Two experimental observations support this notion. First, rhodopsin's catalytic lifetime, at least at constant Ca^{2+}, was not explained by the time required for phosphorylation or arrestin binding (Figs. 7 and 15); thus other processes must contribute to rhodopsin deactivation. Second, the variability of the elementary response increased when phosphorylation was slowed, so that rhodopsin deactivation proceeded effectively as a single step, and this increase in variability was consistent with expectations if the current was fully sensitive to fluctuations in rhodopsin's activity (Fig. 17). Thus reproducibility failed when rhodopsin shut off effectively as a single-step process.

How many steps are required if reproducibility arises from multistep shutoff of rhodopsin's activity? To investigate this we calculated the time-dependent variance for the model described in Eqs. 7 and 10 and a stochastic model in which rhodopsin's activity decayed through a series of transitions. The rate constants of the transitions and activities of the preceding states were constrained so that on average rhodopsin's activity declined exponentially with a 2.5 s time constant. Fig. 18 *B* shows calculations of the time-dependent variance for rhodopsin shutoff through a series of 5, 10, and 20 transitions. Variability in rhodopsin's cumulative activity and in the elementary response decreased as the number of steps was increased. Reducing the variance of the elementary response to the measured level required 10–20 steps.

For multiple steps in rhodopsin shutoff to be effective, the transitions between states should be essentially irreversible. The large free energy difference (~32 kcal/mol) between isomerized, unphosphorylated rhodopsin and the rhodopsin-arrestin complex makes this energetically feasible. If this energy were divided equally among 15 steps, the ratio of forward to backward rate constants for each transition could be 20.

What molecular events might explain 10–20 steps in rhodopsin shutoff? Individual steps could be mediated by interactions of rhodopsin with other molecular species. For example, rhodopsin kinase might initially phosphorylate one of the four sites on the C-terminus, but the kinase might have to rebind to rhodopsin and move the phosphate several times before it reached a site permitting strong arrestin binding. Alternatively, individual steps might represent transitions intrinsic to the rhodopsin molecule. Multiple intrinsic states have been well documented by kinetic studies on ion channels, where the states are thought to represent distinct conformations of the channel protein. In a voltage-gated K^+ channel, for example, there are over 15 distinct

kinetic states (Zagotta et al., 1994). The large number derives partly from independent transitions in the four subunits that form the channel. Although rhodopsin does not consist of subunits, it does contain seven transmembrane helices and four cytoplasmic loops, which are thought to change position after photoisomerization (Farahbakhsh et al., 1995; Altenbach et al., 1996). States of different catalytic activity could conceivably be produced by relative movements of these structures.

Functional role of reproducibility

What biological purpose might be served by reproducible elementary responses? A possible answer is that reproducibility allows the rod to encode the number of active rhodopsin molecules and thus allows accurate estimation of light intensity. However, the accuracy with which the intensity can be estimated will be limited by Poisson fluctuations in the number of photoisomerizations as well as noise intrinsic to the rod, and for all but the dimmest lights Poisson fluctuations dominate. Most of the rod's dark noise is due to thermal isomerization of rhodopsin, which occurs about once every 30 s in a toad rod (Baylor et al., 1980). The requirement that the number of photoisomerizations significantly exceed this number apparently sets the ultimate limit to the sensitivity of rod vision (Aho et al., 1988). The noise variance arising from fluctuations in the elementary response is 20–25 times smaller than that due to Poisson fluctuations. Thus the reproducibility of the elementary response allows the rod to encode the difference between five and six photoisomerizations, whereas Poisson fluctuations in the number of absorbed photons make this difference minimally informative about real differences in light intensity. The elementary response seems "overengineered" for simply estimating light intensity.

Alternatively, reproducibility might preserve information about the times at which photons are absorbed. In a noiseless rod with identical elementary responses, the times of photon absorption could be recovered by unfolding the time course of the elementary response from the observed membrane current. In the real rod, two factors will limit the accuracy of the recovery: fluctuations in the shape of the elementary response (Baylor et al., 1979b) and continuous noise in the transduction cascade (Baylor et al., 1980; Rieke and Baylor, 1996). The contribution of fluctuations in the shape of the elementary response was assessed in the following way. Elementary responses and failures were isolated from an amplitude histogram such as that in Fig. 4. The most likely time of photoisomerization was then estimated from each elementary response by two steps (see Fig. 19, *A* and *B*): 1) the probability of photoisomerization as a function of time was calculated by operating on the photocurrent with a matched filter calculated from the rod's elementary response and continuous dark noise spectrum (Bialek and Owen, 1990); 2) the peak of the time-dependent probability was taken as an estimate of the time of photoisomerization. As the entire rod response was used to make the estimate, the procedure introduced a delay equal to the duration of the elementary response.

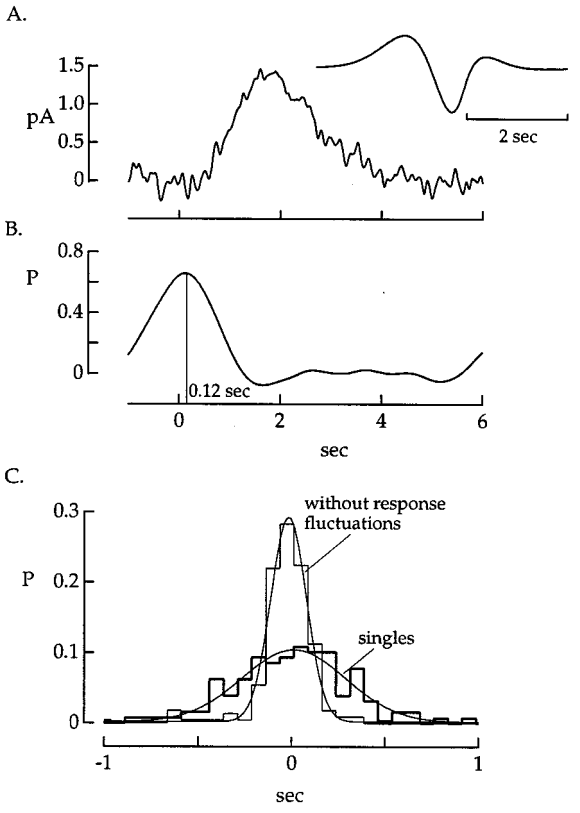

FIGURE 19 The contribution of elementary response fluctuations to the precision of estimated photoisomerization times. (*A*) Response to a single photoisomerization at time $t = 0$ from the experiment of Fig. 3. The time of photoisomerization was estimated from the photocurrent by correcting for the impulse response of the transduction cascade. Without noise it would be possible to recover the time of photoisomerization exactly, but noise introduces some temporal imprecision. The inset shows the impulse response of a filter that takes as input the rod current and produces an estimate of the probability of photoisomerization as a function of time. The filter chosen provides the best estimate of the time-dependent probability of photoisomerization given the single photon response and dark noise (see Bialek and Owen, 1990). The filter utilizes the entire rod response and thus introduces a delay of 6 s in the estimate. (*B*) Time-dependent probability of photoisomerization calculated from single photon response and filter in *A*. The 6-s delay has been removed to facilitate comparison with the actual time of photoisomerization of $t = 0$. The estimated time of photoisomerization was taken as the peak of the time-dependent probability (*vertical line*), which occurred at $t = 0.12$ s in this case. (*C*) Probability densities of estimated times of photoisomerization calculated as in *A* and *B*. The thick trace represents estimates from 129 single photon responses. The Gaussian fitted to the distribution has a standard deviation of 226 ms. Continuous noise and fluctuations in the elementary response contribute to the width of this distribution. The thin trace represents estimates from 223 failures, each with an added stereotyped response (the average of the singles). The Gaussian fitted to this distribution has a standard deviation of 95 ms. This distribution reflects timing errors introduced by continuous noise alone. Comparison of the two distributions indicates that fluctuations in the shape of the elementary response limit the temporal precision of the estimated photon times.

The distribution of estimated photoisomerization times relative to the actual time is shown in Fig. 19 *C* (*thick*

trace), where it is fitted by a Gaussian of standard deviation 275 ms. In results from eight cells the mean standard deviation was 252 ms, so that the imprecision of the time estimate was considerably smaller than the duration of the elementary response. Both response fluctuations and continuous noise contribute to the scatter in the time estimate. To estimate the contribution of continuous noise alone, a stereotyped single photon response was added to the current from each trial in which no photoisomerization occurred and the estimation procedure was repeated. The distribution of these estimated times is shown by the thin trace in Fig. 19 *C*, where it is fitted by a Gaussian of standard deviation 95 ms. In eight cells the mean standard deviation was 118 ms, considerably smaller than the estimate of 252 ms from the actual elementary responses. The conclusion is that fluctuations in the shape of the elementary response limit the precision with which photoisomerization times can be estimated.

The analysis above indicates that the temporal precision of operations in the rod pathways would suffer if reproducibility of the elementary response failed. This temporal precision may be critical for tasks such as correctly identifying the direction of motion of a visual stimulus or correctly identifying an object that suddenly appears in the visual field.

We thank Drs. E. J. Chichilnisky, B. Hille, and M. Meister for careful reading of the manuscript; W. Bialek, Y. Koutalos, and L. Stryer for stimulating discussions; and Robert Schneeveis for excellent technical assistance.

This work was supported by the National Eye Institute through grants EY01543 (to DAB) and EY11850 (to FR).

REFERENCES

Aho, A.-C., K. Donner, C. Hydèn, L. O. Larsen, and T. Reuter. 1988. Low retinal noise in animals with low body temperature allows high visual sensitivity. *Nature.* 334:348–350.

Altenbach, C., K. Yang, D. L. Farrens, Z. T. Farahbakhsh, H. G. Khorana, and W. L. Hubbell. 1996. Structural features and light-dependent changes in the cytoplasmic interhelical E-F loop region of rhodopsin: a site-directed spin-labeling study. *Biochemistry.* 35:12470–12478.

Arshavsky, V. Yu., and M. D. Bownds. 1992. Regulation of deactivation of photoreceptor G protein by its target enzyme and cGMP. *Nature.* 357: 416–417.

Baylor, D. A., T. D. Lamb, and K.-W. Yau. 1979a. The membrane current of single rod outer segments. *J. Physiol. (Lond.).* 288:589–611.

Baylor, D. A., T. D. Lamb, and K.-W. Yau. 1979b. Responses of retinal rods to single photons. *J. Physiol. (Lond.).* 288:613–634.

Baylor, D. A., G. Matthews, and K.-W. Yau. 1980. Two components of electrical dark noise in toad retinal rod outer segments. *J. Physiol. (Lond.).* 309:591–621.

Baylor, D. A., B. J. Nunn, and J. L. Schnapf. 1984. The photocurrent, noise and spectral sensitivity of rods of the monkey *Macaca fascicularis*. *J. Physiol. (Lond.).* 357:575–607.

Bennett, N., and A. Sitaramayya. 1988. Inactivation of photoexcited rhodopsin in retinal rods: the roles of rhodopsin kinase and 48-kDa protein (arrestin). *Biochemistry.* 27:1710–1715.

Bialek, W., and W. G. Owen. 1990. Temporal filtering in retinal bipolar cells: elements of an optimal computation? *Biophys. J.* 58:1227–1233.

Cervetto, L., L. Lagnado, R. J. Perry, D. W. Robinson, and P. A. McNaughton. 1989. Extrusion of calcium from rod outer segments is driven by both sodium and potassium gradients. *Nature.* 337:740–743.

Chen, J., C. L. Makino, N. S. Peachey, D. A. Baylor, and M. I. Simon. 1995. Mechanisms of rhodopsin inactivation in vivo as revealed by a COOH-terminal truncation mutant. *Science.* 267:374–377.

Corson, D. W., M. C. Cornwall, and D. R. Pepperberg. 1994. Evidence for the prolonged photoactivated lifetime of an analogue visual pigment containing 11-*cis*-9-desmethylretinal. *Vis. Neurosci.* 11:91–98.

Erickson, M. A., L. Lagnado, S. Zozulya, T. A. Neubert, L. Stryer, and D. A. Baylor. 1998. The effect of recombinant recoverin on the photoresponse of truncated rod photoreceptors. *Proc. Natl. Acad. Sci. USA.* 95:6474–6479.

Farahbakhsh, Z. T., K. D. Ridge, H. G. Khorana, and W. L. Hubbell. 1995. Mapping light-dependent structural changes in the cytoplasmic loop connecting helices C and D in rhodopsin: a site-directed spin labeling study. *Biochemistry.* 34:8812–8819.

Fung, B. K. 1983. Characterization of transducin from bovine retinal rod outer segments. I. Separation and reconstitution of the subunits. *J. Biol. Chem.* 258:10495–10502.

Gray-Keller, M. P., and P. B. Detwiler. 1994. The calcium feedback signal in the phototransduction cascade of vertebrate rods. *Neuron.* 13: 849–861.

Hecht, S., S. Shlaer, and M. Pirenne. 1942. Energy, quanta and vision. *J. Gen. Physiol.* 25:819–840.

Karpen, J. W., A. L. Zimmerman, L. Stryer, and D. A. Baylor. 1988. Gating kinetics of the cyclic-GMP-activated channel of retinal rods: flash photolysis and voltage-jump studies. *Proc. Natl. Acad. Sci. USA.* 85:1287–1291.

Kawamura, S. 1993. Rhodopsin phosphorylation as a mechanism of cyclic GMP phosphodiesterase regulation by S-modulin. *Nature.* 362: 855–857.

Koch, K. W., and L. Stryer. 1988. Highly cooperative feedback control of retinal rod guanylate cyclase by calcium ions. *Nature.* 334:64–66.

Koutalos, Y., K. Nakatani, T. Tamura, and K.-W. Yau. 1995a. Characterization of guanylate cyclase activity in single retinal rod outer segments. *J. Gen. Physiol.* 106:863–890.

Koutalos, Y., K. Nakatani, and K.-W. Yau. 1995b. The cGMP-phosphodiesterase and its contribution to sensitivity regulation in retinal rods. *J. Gen. Physiol.* 106:891–921.

Koutalos, Y., and K.-W. Yau. 1996. Regulation of sensitivity in vertebrate rod photoreceptors by calcium. *Trends Neurosci.* 19:73–81.

Krupnick, J. G., V. V. Gurevich, and J. L. Benovic. 1997. Mechanism of quenching of phototransduction. Binding competition between arrestin and transducin for phosphorhodopsin. *J. Biol. Chem.* 272:18125–18131.

Lagnado, L., and D. A. Baylor. 1992. Signal flow in visual transduction. *Neuron.* 8:995–1002.

Lagnado, L., and D. A. Baylor. 1994. Calcium controls light-triggered formation of catalytically active rhodopsin. *Nature.* 367:273–277.

Langlois, G., C. K. Chen, K. Palczewski, J. B. Hurley, and T. M. Vuong. 1996. Responses of the phototransduction cascade to dim light. *Proc. Natl. Acad. Sci. USA.* 93:4677–4682.

Lyubarsky, A., S. Nikonov, and E. N. Pugh. 1996. The kinetics of inactivation of the rod phototransduction cascade with constant Ca_i^{2+}. *J. Gen. Physiol.* 107:19–34.

Matthews, H. R., R. L. W. Murphy, G. L. Fain, and T. D. Lamb. 1988. Photoreceptor light adaptation is mediated by cytoplasmic calcium concentration. *Nature.* 334:67–69.

McCarthy, S. T., J. P. Younger, and W. G. Owen. 1996. Dynamic spatially non-uniform calcium regulation in frog rods exposed to light. *J. Neurophysiol.* 76:1991–2004.

Miller, J. L., and E. A. Dratz. 1984. Phosphorylation at sites near rhodopsin's carboxyl-terminus regulates light initiated cGMP hydrolysis. *Vision Res.* 24:1509–1521.

Murnick, J. G., and T. D. Lamb. 1996. Kinetics of desensitization induced by saturating flashes in toad and salamander rods. *J. Physiol. (Lond.).* 495:1–13.

Nakatani, K., and K.-W. Yau. 1988a. Calcium and light adaptation in retinal rods and cones. *Nature.* 334:69–71.

Nakatani, K., and K.-W. Yau. 1988b. Calcium and magnesium fluxes across the plasma membrane of the toad rod outer segment. *J. Physiol. (Lond.).* 395:695–729.

Nakatani, K., and K.-W. Yau. 1988c. Guanosine 3′,5′-cyclic monophosphate-activated conductance studied in a truncated rod outer segment of the toad. *J. Physiol. (Lond.).* 395:731–753.

Nikonov, S., N. Enghet, and E. N. Pugh. 1998. Kinetics of recovery of the dark-adapted salamander rod photoresponse. *J. Gen. Physiol.* 111:7–37.

Ohguro, H., J. P. Van-Hooser, A. H. Milam, and K. Palczewski. 1995. Rhodopsin phosphorylation and dephosphorylation in vivo. *J. Biol. Chem.* 270:14259–14262.

Palczewski, K., G. Rispoli, and P. B. Detwiler. 1992. The influence of arrestin (48K protein) and rhodopsin kinase on visual transduction. *Neuron.* 8:117–126.

Pepperberg, D. R., J. Jin, and G. J. Jones. 1994. Modulation of transduction gain in light adaptation of retinal rods. *Vis. Neurosci.* 11:53–62.

Pugh, E. N., Jr., and T. D. Lamb. 1993. Amplification and kinetics of the activation steps in phototransduction. *Biochim. Biophys. Acta.* 1141: 111–149.

Rieke, F., and D. A. Baylor. 1996. Molecular origin of continuous dark noise in rod photoreceptors. *Biophys. J.* 71:2553–2572.

Rispoli, G., W. A. Sather, and P. B. Detwiler. 1993. Visual transduction in dialysed detached rod outer segments from lizard retina. *J. Physiol. (Lond.).* 465:513–537.

Sagoo, M. S., and L. Lagnado. 1997. G-protein deactivation is rate-limiting for shut-off of the phototransduction cascade. *Nature.* 389:392–395.

Sakitt, B. 1972. Counting every quantum. *J. Physiol. (Lond.).* 223:131–150.

Schnapf, J. L. 1983. Dependence of the single photon response on longitudinal position of absorption in toad rod outer segments. *J. Physiol. (Lond.).* 343:147–159.

Torre, V., H. R. Matthews, and T. D. Lamb. 1986. Role of calcium in regulating the cyclic GMP cascade of phototransduction in retinal rods. *Proc. Natl. Acad. Sci. USA.* 83:7109–7113.

van der Velden, H. A. 1946. The number of quanta necessary for the perception of light in the human eye. *Opthalmologica.* 111:321–331.

Xu, J., R. L. Dodd, C. L. Makino, M. I. Simon, D. A. Baylor, and J. Chen. 1997. Prolonged photoresponses in transgenic mouse rods lacking arrestin. *Nature.* 389:505–509.

Yau, K.-W., and K. Nakatani. 1985. Light-suppressible, cyclic GMP-sensitive conductance in the plasma membrane of a truncated rod outer segment. *Nature.* 317:252–255.

Zagotta, W. N., T. Hoshi, and R. W. Aldrich. 1994. Shaker potassium channel gating. III. Evaluation of kinetic models for activation. *J. Gen. Physiol.* 103:321–362.

Zimmerman, A. L., and D. A. Baylor. 1986. Cyclic GMP-sensitive conductance of retinal rods consists of aqueous pores. *Nature.* 321:70–72.